Received: 12 July 2018 | Revised: 09 November 2018 | Accepted: 16 November 2018 | Published on: 15 January 2019

DOI: 10.1002/qj.3438

RESEARCH ARTICLE

Quarterly Journal of the Royal Meteorological Society RMetS

Estimation of physical parameters under location uncertainty using an ensemble^2–expectation–maximization algorithm

Yin Yang[1] | Etienne Mémin[2]

[1]Irstea, UR OPAALE, Rennes Cedex, France
[2]Inria, Fluminance Group, Campus Universitaire de Beaulieu, Rennes Cedex, France

Correspondence
Yin Yang, Irstea, UR OPAALE, F-35044 Rennes Cedex, France.
Email: iamyangyin@gmail.com

Estimating the parameters of geophysical dynamic models is an important task in the data assimilation (DA) techniques used to forecast initialization and reanalysis. In the past, most parameter estimation strategies were derived by state augmentation, yielding algorithms that are easy to implement but may exhibit convergence difficulties. The expectation–maximization (EM) algorithm is considered advantageous because it employs two iterative steps to estimate the model state and the model parameter separately. In this work, we propose a novel ensemble formulation of the maximization step in EM that allows a direct optimal estimation of the physical parameters using iterative methods for linear systems. This departs from current EM formulations that are only capable of dealing with additive model error structures. This contribution shows how the EM technique can be used for dynamics identification problems with the model error parameterized as an arbitrary complex form. The proposed technique is used here for the identification of stochastic subgrid terms that account for processes unresolved by a geophysical fluid model. This method, together with the augmented state technique, is evaluated to estimate such subgrid terms through high-resolution data. As compared to the augmented state technique, our method is shown to yield considerably more accurate parameters. In addition, in terms of prediction capacity, it leads to a smaller generalization error as a result of the overfitting of the trained model on the presented data and eventually better forecasts.

KEYWORDS

data assimilation, expectation–maximization algorithm, parameter estimation, stochastic modelling

1 | INTRODUCTION

Parameter estimation is an important aspect of data assimilation (DA) techniques. Traditionally, the same estimation scheme is employed for both state and parameter estimation through the so-called augmented state technique. This technique consists in encapsulating the entire set of unknown parameters into an augmented state vector, which is then jointly estimated. Such work has been pioneered by Navon (1998) in the context of variational methods and extended by Anderson (2001) to ensemble methods.

One of the most crucial parameters for the forecast or analysis of geophysical flow is related to the inescapable lack of representativeness of the dynamics model. Those errors come from approximations made in the analytical constitution stages of the models and are dictated by practical computational constraints. They may also ensue from a lack of physical information on the complex small-scale processes involved. The action on the large-scale (resolved) components of these unresolved processes must be properly modelled; they are usually qualified under the term "subgrid model." These models do not generally rely on rigorous theoretical grounds and are often defined to mimic qualitative descriptions of turbulence or the small-scale effect.

Recently, Mémin (2014) and Holm (2015) proposed a stochastic dynamics approach to model the unresolved

small-scale components. The basic idea is to consider the stochastic nature of flow from the start of the physical modelling process in order to directly derive the governing physical dynamical system driven by stochastic processes. In these approaches, recovering the subgrid-scale errors boils down to the calibration of a variance tensor representing the fast-changing fluctuation associated with turbulence. Nowadays, observation snapshots can reach resolutions that are much finer than the model grid resolution. As a consequence, the question of the ability to estimate the subgrid parameters from high-resolution observations immediately arises.

In this study, we investigate such an estimation problem. We rely on a reconstruction basis formulated by coupling a stochastic modelling process (Mémin, 2014) and relevant data through an optimal estimation scheme. Recently, Yang and Mémin (2017) demonstrated an implementation of the augmented state strategy by applying an ensemble optimal control (EnVar) method to this state/parameter estimation problem. The authors found that although the state estimated from the joint distribution can be quite accurate due to the enlarged ensemble spread induced by the stochastic dynamics representation, the estimated parameter field tends to be much less accurate, with an underestimation of the reference values. As a result, the parameter field needs to be retuned by ad hoc inflation techniques to avoid model blow-up and/or covariance collapse. Model blow-up results from strong, uncontrolled numerical instabilities of the dynamical model, while ensemble collapsing corresponds to ensemble members with no variabilities. In particular, an insufficient spread of the ensemble prevents any accurate estimation of the probability density functions involved in the Bayesian inference process.

In this paper, we devise an expectation–maximization (EM) algorithm to overcome the described shortcomings associated with augmented-state-based techniques. Our motivation for using the EM algorithm is twofold. Within a Bayesian framework, we want both to propose an elegant and flexible solution for estimating the state and the model parameters separately and to provide a numerically stable formulation for maximizing the likelihood. Eventually, highly accurate stochastic parameters associated with the stochastic modelling process can be obtained, leading to better reconstruction and prediction of the state.

Before describing the proposed approach in detail, we briefly review the principles of the EM technique. In the statistical literature, the EM algorithm (McLachlan and Krishnan, 2007) is an efficient parameter estimation algorithm aimed at finding the maximum likelihood solution of a system containing latent variables. The latent variables (or hidden states) refer to non-observed variables that are usually introduced to facilitate the modelling process. The maximum likelihood (ML) estimation of the parameter $\boldsymbol{\theta}$ given observations $\mathbf{y}$ consists in finding $\boldsymbol{\theta}$ so that the conditional probability $p(\mathbf{y}|\boldsymbol{\theta})$ reaches its maximum. For systems without latent variables, such estimations can be directly solved by employing Newton-type methods.

In terms of dynamical systems with latent variables $\mathbf{x}$, the ML function $p(\mathbf{y}|\boldsymbol{\theta})$ is given by marginalizing the complete joint likelihood function $p(\mathbf{y},\mathbf{x}|\boldsymbol{\theta})$ over $\mathbf{x}$:

$$\ln p(\mathbf{y}|\boldsymbol{\theta}) = \ln \sum_{\mathbf{x}} p(\mathbf{y},\mathbf{x}|\boldsymbol{\theta}). \tag{1}$$

Maximizing the likelihood can be difficult; instead, it appears easier to maximize its lower bound. Introducing an arbitrary probability distribution $q(\mathbf{x})$,

$$\begin{aligned}\ln p(\mathbf{y}|\boldsymbol{\theta}) &= \ln \sum_{\mathbf{x}} q(\mathbf{x}) \frac{p(\mathbf{y},\mathbf{x}|\boldsymbol{\theta})}{q(\mathbf{x})} \\ &\geq \sum_{\mathbf{x}} q(\mathbf{x}) \ln \frac{p(\mathbf{y},\mathbf{x}|\boldsymbol{\theta})}{q(\mathbf{x})} \triangleq \mathcal{L}(q,\boldsymbol{\theta}),\end{aligned} \tag{2}$$

where the inequality showing that the last term $\mathcal{L}(q,\boldsymbol{\theta})$ is the lower bound of $\ln p(\mathbf{y}|\boldsymbol{\theta})$ follows from Jensen's inequality. The EM principle is then built from a two-stage coordinate ascent procedure. At iteration $l+1$, in the first step, referred to as the *expectation* step (the E-step), it can be proven that when setting $q_{l+1}(\mathbf{x})$ to the posterior conditional distribution $p(\mathbf{x}|\mathbf{y},\boldsymbol{\theta}_l)$, the functional $\mathcal{L}(q,\boldsymbol{\theta}_l)$ is maximized. This step can be interpreted as achieving the fixed lower bound $\mathcal{L}(q,\boldsymbol{\theta}_l)$ predetermined through $\boldsymbol{\theta}_l$. Interested readers may refer to Jordan (2003) and Bishop (2006) for a proof based on Kullback–Leibler (KL) divergence. In the second step, referred to as the *maximization* step (the M-step), we start by substituting $q_{l+1}(\mathbf{x}) = p(\mathbf{x}|\mathbf{y},\boldsymbol{\theta}_l)$ into $\mathcal{L}(q,\boldsymbol{\theta})$:

$$\begin{aligned}\mathcal{L}(q_{l+1},\boldsymbol{\theta}_{l+1}) &= \sum_{\mathbf{x}} p(\mathbf{x}|\mathbf{y},\boldsymbol{\theta}_l) \ln p(\mathbf{y},\mathbf{x}|\boldsymbol{\theta}_{l+1}) \\ &\quad - \sum_{\mathbf{x}} p(\mathbf{x}|\mathbf{y},\boldsymbol{\theta}_l) \ln p(\mathbf{x}|\mathbf{y},\boldsymbol{\theta}_l).\end{aligned} \tag{3}$$

Since the second term is independent of $\boldsymbol{\theta}_{l+1}$, only the first term, the expectation of the log joint distribution with respect to the posterior conditional distribution, needs to be considered in the maximization step. Consequently, we search for

$$\boldsymbol{\theta} = \arg\max_{\boldsymbol{\theta}} \mathcal{Q}(\boldsymbol{\theta},\boldsymbol{\theta}_l), \tag{4}$$

where $\mathcal{Q}$ is defined by

$$\mathcal{Q}(\boldsymbol{\theta},\boldsymbol{\theta}_l) = \sum_{\mathbf{x}} p(\mathbf{x}|\mathbf{y},\boldsymbol{\theta}_l) \ln p(\mathbf{y},\mathbf{x}|\boldsymbol{\theta}). \tag{5}$$

This step can also be interpreted as finding $\boldsymbol{\theta}_{l+1}$ to increase the lower bound $\mathcal{L}(q_{l+1},\boldsymbol{\theta}_{l+1})$. Thus we iterate over the two consecutive steps in order to increase the original likelihood function gradually. This iterative procedure is pursued until a convergence criterion is satisfied – usually set to a small constant threshold of the change of $\boldsymbol{\theta}$ between two consecutive iterations. Although the EM algorithm is guaranteed to iteratively increase the likelihood function, approximate computation in the E-step and/or M-step instead of the exact solutions may hinder global convergence in practice/theory.

Several comments can be made by comparing the above EM formulation to other data assimilation approaches. First, we notice that the latent variables, corresponding to the

internal states, are imperative and crucial in the dynamics modelling process because they reflect intrinsic mechanisms of the studied phenomenon. Second, typical DA schemes seek to estimate the posterior conditional distribution of the latent variable $\mathbf{x}$. This indeed corresponds to the expectation step in the EM algorithm. Lastly, the augmented state technique treats both the parameters and the state on an equal footing as random variables – which is totally correct in the Bayesian context – however, the state and the parameters are usually of different natures. Indeed, the hidden state is generated by the dynamical model, while the dynamics itself is known only up to the value of the parameters. On the other hand, the EM algorithm enables one to build two separate estimation procedures for the state and the parameters, respectively. Yet, this is done in a consistent Bayesian framework. Here the term "consistent" is used to describe the synchronous and compatible relationships between two objective distributions for estimating the state and the parameters, respectively, from a time sequence of data. From a statistical perspective, the augmented state technique tries to find the state/parameters by maximizing the posterior joint conditional probability function $p(\mathbf{x}, \boldsymbol{\theta}|\mathbf{y})$, while the EM algorithm works on the marginalized likelihood instead. Searching for the augmented state is conceptually easy to implement but can pose practical optimization problems because the state and the parameter may differ by orders of magnitude. This generally requires the use of a proper scaling technique in the optimization. The joint optimization procedure can be decoupled into two separate optimization procedures for the state and the parameters. This decoupled strategy, forming the dual-filter approach, is, despite its simplicity, likely to produce inconsistent state and parameter estimations. Also, the augmented state technique fails to estimate the stochastic parameters (e.g., model error covariance matrix $\mathbf{Q}$) (Delsole and Yang, 2010). This is related to the parameter identifiability problem due to the lack of correlation between the state and the parameters. Augmented state techniques have their own advantages in terms of easily building the covariance information. However, this is also their main weakness. When the considered parameter has a spatial structure, the size of the covariance matrix increases quadratically with the size of the parameter. In the EM algorithm, however, the parameter covariance is not needed. Due to the complexity of the optimization procedure (e.g., associated with a low-rank covariance matrix), the augmented state method is known to exhibit instability issues yielding model blow-up or ensemble collapse phenomena as discussed earlier. Even if the inference problem can be solved smoothly, the added number of degrees of freedom associated with the parameters may lead to a so-called overfitted model, which is too sensitive to the observation noise.

Recent advances in the integration of the EM algorithm into data assimilation are exemplified in the work of Dreano *et al.* (2017) and Pulido *et al.* (2018). Their work is focused on the estimation of a low-rank model error covariance term associated with a reduced-order noisy dynamics. The form of the noise term has been set empirically. Such an empirical form for the randomization of the dynamical system, which appears to be innocent at first glance, may in fact be problematic. The energy intake due to the increase in variance brought by the noise model is not compensated for by any dissipation mechanism. This imbalance may lead to numerical instability and to the breaking of physical conservation laws, as the variance may increase in an uncontrolled way. In addition, a non-physical random forcing (i.e., with a form that does not ensue from a physical conservation law) may lead to random dynamics whose low-noise limit differs significantly from the deterministic original system (Chapron *et al.*, 2018). In other words, the random dynamics converges poorly to the deterministic system for low noise.

In this work, we investigate a different objective that consists in estimating a model parameter ensuing from a rigorous random representation of geophysical fluid dynamics. We show in particular how the estimation of such parameters is indeed tractable using an iterative ensemble-based EM algorithm. To this end, we begin with a brief review on how the effect of small-scale oscillations exerted on large-scale dynamics is naturally introduced through a stochastic transportation principle, followed by a formal introduction of the EM algorithm in the context of DA. We later present the EnRTS smoother, which is used in the state estimation stage of the EM algorithm. We then focus on the ensemble-based EM algorithm that allows the physical parameters to be explicitly estimated. A detailed comparative study of our proposed EM-based parameter estimation scheme with the EM as used in Dreano *et al.* (2017) and the ML as used in Pulido *et al.* (2018) is presented in Section 6. In this section, we also compared our method with two closely related approaches: one by Delsole and Yang (2010), in which the generalized ML approach combined with the dual Kalman filter is employed to estimate the state and the parameter separately, and another by Ueno and Nakamura (2016), in which EM is used with a Gaussian mixture observation model represented by samples to estimate the observation error covariance matrix. We conclude with results of numerical assessments and related discussions.

2 | LOCATION UNCERTAINTY MODELLING RELATED TO SCALE DISCREPANCY

The location uncertainty principle is primarily based on the decomposition of the fluid particle displacements as

$$\boldsymbol{X}_t = \boldsymbol{X}_{t_0} + \int_{t_0}^{t} \boldsymbol{w}(\boldsymbol{X}_s, s)\mathrm{d}s + \int_{t_0}^{t} \boldsymbol{\sigma}(\boldsymbol{X}_s, s)\mathrm{d}\boldsymbol{B}_s, \qquad (6)$$

with $\boldsymbol{X}_t$ denoting the flow map at time t, $\boldsymbol{w}$ the velocity of the smooth fluid particles corresponding to the sought "large-scale" solution, and $\mathrm{d}\boldsymbol{B}_t$ a d-dimensional Wiener increment ($d = 2, 3$) function. The term $\boldsymbol{\sigma}(x, t)\mathrm{d}\boldsymbol{B}_t$ represents the

fast-changing fluctuation associated with turbulence; it has a much lower time-scale than $\boldsymbol{w}$, the smooth component. This term is defined from an integral operator of the Brownian function over the fluid domain Ω:

$$(\sigma(x,t)\mathrm{d}\boldsymbol{B}_t)^i = \int_\Omega \sum_j \sigma^{ij}(x,y,t)\mathrm{d}\boldsymbol{B}_t^j(y)\mathrm{d}y. \tag{7}$$

Both $\boldsymbol{\sigma}$ and $\boldsymbol{w}$ need to be solved or modelled. Stochastic Navier–Stokes equations can be deduced by considering a stochastic representation of the Reynolds transport theorem (RTT) (Mémin, 2014) through variational principle (Holm, 2015) or homogenization techniques (Cotter *et al.*, 2017). The stochastic representation of RTT introduces meaningful terms for turbulence modelling. It includes (a) a diffusion term that represents the mixing of the large-scale component with the small-scale random field; (b) a modified large-scale advection describing the statistical action of the turbulence inhomogeneity on the large-scale drift; and (c) a multiplicative random term depicting the transport of the large-scale component by the small-scale random component. The variance increase brought by this latter term is in equilibrium with the amount of diffusion associated with the first term (Resseguier *et al.*, 2017a). The inhomogeneous diffusion term can be seen as a generalization of classical eddy-viscosity subgrid models. The modified advection term corresponds to a noise-induced velocity term, which drives the fluid particles from the turbulent region of high variance toward more quiescent areas with minimum variance. Finally, the multiplicative advection random process describes well the shape of the non-Gaussian probability distribution function associated with turbulent flows, with a fat tail emerging from the turbulence intermittency (Kraichnan, 1968; 1994; Majda and Kramer, 1999; Sura *et al.*, 2005).

The modelling under location uncertainty has been used to derive stochastic expressions of geophysical flows (Resseguier *et al.*, 2017a; 2017b; 2017c), efficient reduced-order flow models (Resseguier *et al.*, 2017d; Chapron *et al.*, 2018), and large eddy simulation models for various types of flows (Kadri Harouna and Mémin, 2017; Chandramouli *et al.*, 2018).

In this article we focus on the shallow-water model under location uncertainty. In the following we give the one-dimensional stochastic shallow water directly in terms of the depth h, the free surface $\eta = h + b$, with b the bottom height, and the velocity u. For a complete description of the model derivation, please refer to Yang and Mémin (2017).

$$\mathrm{d}_t h + \Big(\partial_x\big(h\underbrace{(u - \frac{1}{2}\partial_x a_{xx})}_{\tilde{u}}\big) - \frac{1}{2}\partial_x(a_{xx}\partial_x h)\Big)dt + \partial_x h(\sigma d\boldsymbol{B_t})_x = 0, \tag{8a}$$

$$\mathrm{d}_t(hu) + \Big(\partial_x\Big(hu\tilde{u} + \frac{1}{2}g\eta^2\Big) - \frac{1}{2}\partial_x\big(a_{xx}\partial_x(hu)\big) + a_{xx}\partial_x h\partial_x u\Big)\mathrm{d}t + u\partial_x h(\sigma\mathrm{d}\boldsymbol{B_t})_x = 0. \tag{8b}$$

The system 8 is essentially made up of stochastic partial differential equations. Besides the fast fluctuation part associated with the Wiener increment $\mathrm{d}\boldsymbol{B_t}$, extra terms associated with the variance tensor $\boldsymbol{a}$ are also included. This quantity is directly related to the variance of the small-scale component as it is defined from the diagonal of the uncertainty covariance:

$$\boldsymbol{a}(\boldsymbol{x},t)\delta(t-t')\mathrm{d}t = \mathbb{E}\left((\boldsymbol{\sigma}(\boldsymbol{x},t)\mathrm{d}\boldsymbol{B}_t)\left(\boldsymbol{\sigma}(\boldsymbol{x},t')\mathrm{d}\boldsymbol{B}_{t'}\right)^T\right). \tag{9}$$

3 | AN EM ALGORITHM FOR MODEL PARAMETER ESTIMATION

The data assimilation problem can be formulated under a state-space model framework. A general continuous evolution model can be described by a discrete Markovian nonlinear state mapping operator:

$$\mathbf{x}_k = \varphi_k(\mathbf{x}_{k-1}, \boldsymbol{a}) + \boldsymbol{\xi}_k, \tag{10}$$

where k is the time index. The unknown initial condition is modelled by

$$\mathbf{x}_0 = \mathbf{x}_0^f + \boldsymbol{\omega}_k, \tag{11}$$

where the superscript f refers to the *forecast*, indicating prior knowledge about the initial condition, combined with the observation equation

$$\mathbf{y}_k = \mathbb{H}(\mathbf{x}_k) + \boldsymbol{\epsilon}_k, \tag{12}$$

which links the observation $\mathbf{y} \in \mathbb{R}^m$ and the state $\mathbf{x} \in \mathbb{R}^n$ by means of a nonlinear operator $\mathbb{H}$. The observations are assumed to be mutually conditionally independent. The noise may depend on the state but is assumed to be Gaussian when conditioned on the state: $\boldsymbol{\xi}_{|x} \propto \mathcal{N}(0, \mathbf{Q})$, $\boldsymbol{\omega}_{|x} \propto \mathcal{N}(0, \mathbf{P}_0)$ and $\boldsymbol{\epsilon}_{|x} \propto \mathcal{N}(0, \mathbf{R})$. For the remainder of the paper, we denote the length of the observational time sequences by K and the parameter set $(\boldsymbol{a}, \mathbf{x}_0^f, \mathbf{Q}, \mathbf{P}_0, \mathbf{R})$ by $\boldsymbol{\theta}$.

Note the following remarks on systems 10, 11 and 12:

- Although any parameters contributing to φ_k and $\mathbb{H}$ could also be identified by the EM algorithm, in this paper we consider that all error sources in φ_k are attributed to the variance tensor $\boldsymbol{a}$. We will nevertheless show in Section 6.3 how to estimate the observation covariance $\mathbf{R}$.
- We still assume unimodal Gaussian errors because such an assumption leads to simple and efficient estimation algorithms. To represent arbitrary non-Gaussian error distributions, a Gaussian mixture model can be employed in terms of either system 10, 11 or 12 (Sondergaard and Lermusiaux, 2013). They are not harder to deal with, although additional approximative estimation methods must be introduced to estimate the mixing coefficients.

To find the optimal $\boldsymbol{\theta}$, the EM algorithm proceeds as follows. In the E-step, a state estimation problem is performed, as suggested in Section 1, by computing the posterior conditional distribution $p(\mathbf{x}_{0:K}|\mathbf{y}_{1:K}, \boldsymbol{\theta}_l)$. Consequently, in the

M-step, we look for $\boldsymbol{\theta}_{l+1}$ maximizing $\mathcal{Q}(\boldsymbol{\theta}_{l+1}, \boldsymbol{\theta}_l)$. Since we are dealing with time-sequential data, we rewrite its definition as

$$\mathcal{Q}(\boldsymbol{\theta}_{l+1}, \boldsymbol{\theta}_l) = \int p(\mathbf{x}_{0:K}|\mathbf{y}_{1:K}, \boldsymbol{\theta}_l) \ln p(\mathbf{y}_{1:K}, \mathbf{x}_{0:K}|\boldsymbol{\theta}) \mathrm{d}\mathbf{x}. \quad (13)$$

A classical Bayesian manipulation of $\ln p(\mathbf{y}_{1:K}, \mathbf{x}_{0:K}|\boldsymbol{\theta})$, with the Markov property of the dynamics and the conditional independence of the observations with respect to the state, leads to

$$\ln p(\mathbf{y}_{1:K}, \mathbf{x}_{0:K}|\boldsymbol{\theta}_{l+1}) = \ln p(\mathbf{x}_0) + \sum_{k=1}^{K} \ln p(\mathbf{x}_k|\mathbf{x}_{k-1}, \boldsymbol{\theta}_{l+1}) + \sum_{k=1}^{K} \ln p(\mathbf{y}_k|\mathbf{x}_k, \boldsymbol{\theta}_{l+1}). \quad (14)$$

Substituting this formula into Equation 13 yields

$$\mathcal{Q} = \underbrace{\int p(\mathbf{x}_0|\mathbf{y}_{1:K}, \boldsymbol{\theta}_l) \ln p(\mathbf{x}_0) \mathrm{d}\mathbf{x}_0}_{\mathcal{Q}_1} + \underbrace{\sum_{k=1}^{K} \int p(\mathbf{x}_k, \mathbf{x}_{k-1}|\mathbf{y}_{1:K}, \boldsymbol{\theta}_l) \ln p(\mathbf{x}_k|\mathbf{x}_{k-1}, \boldsymbol{\theta}_{l+1}) \mathrm{d}\mathbf{x}_k \mathrm{d}\mathbf{x}_{k+1}}_{\mathcal{Q}_2} + \underbrace{\sum_{k=0}^{K} \int p(\mathbf{x}_k|\mathbf{y}_{1:K}, \boldsymbol{\theta}_l) \ln p(\mathbf{y}_k|\mathbf{x}_k, \boldsymbol{\theta}_{l+1}) \mathrm{d}\mathbf{x}_k}_{\mathcal{Q}_3}. \quad (15)$$

Introducing the state-space model (Equations 10–12), we have

$$\mathcal{Q}_1 = -\frac{1}{2} \ln |\mathbf{P}_0| - \mathcal{E}_{\mathbf{x}_0|\mathbf{y}_{1:K}, \boldsymbol{\theta}_l} \left\{ \frac{1}{2} \|\mathbf{x}_0 - \mathbf{x}_0^f\|^2_{\mathbf{P}_0} \right\}, \quad (16)$$

$$\mathcal{Q}_2 = -\frac{K-1}{2} \ln |\mathbf{Q}| - \mathcal{E}_{\mathbf{x}_{k,k-1}|\mathbf{y}_{1:K}, \boldsymbol{\theta}_l} \left\{ \frac{1}{2} \sum_{k=1}^{K} \|\mathbf{x}_k - \varphi_k(\mathbf{x}_{k-1}, \boldsymbol{a}_{l+1})\|^2_{\mathbf{Q}} \right\}, \quad (17)$$

$$\mathcal{Q}_3 = -\frac{K}{2} \ln |\mathbf{R}| - \mathcal{E}_{\mathbf{x}_k|\mathbf{y}_{1:K}, \boldsymbol{\theta}_l} \left\{ \frac{1}{2} \sum_{k=0}^{K} \|\mathbf{y}_k - \mathbb{H}(\mathbf{x}_k)\|^2_{\mathbf{R}} \right\}, \quad (18)$$

where $\mathcal{E}_X(f)$ denotes the expectation of f with respect to the law of X and we omit the constant terms. We note the Mahalanobis norm $\|f\|^2_A = (f, A^{-1}f)$, in which A^{-1} is an inverse covariance matrix and f, g is the L^2 inner product. Note that closed-form solutions can be found for parameters such as $\mathbf{x}_0^f, \mathbf{P}_0, \mathbf{R}$ by setting the derivative of $\mathcal{Q}$ with respect to the corresponding parameters to zero. Readers may refer to Bishop (2006) for solutions with linear models or to Dreano *et al.* (2017) when ensemble approximations of nonlinear models are introduced. Our approach differs because, first of all, we want to directly obtain a point estimation of the physical parameter $\boldsymbol{a}$ and not an estimation through some compensating error covariances; secondly, our approach can yield the re-estimation for the model error covariance $\mathbf{Q}$, similarly to standard EM approaches, but also extends the scenario to the case where $\mathbf{Q}$ is related to $\boldsymbol{a}$. Due to the (usual) nonlinear nature of the flow map, no closed-form solution exists. The standard procedure for maximizing the cost function with respect to parameters of nonlinear autoregressive models given one-dimensional time series is provided in Nelson (2000) and Haykin (2004). Here, we reformulate the scheme to deal with parameters involved in a complex nonlinear dynamic model of large spatial resolution, and we devise an iterative formulation relying on an ensemble approximation of the parameter-related tangent linear model. For the rest of this section, we will exhibit simpler forms of $\mathcal{Q}_1$, $\mathcal{Q}_2$ and $\mathcal{Q}_3$ by applying the expectation operation inside the sum operator. The principle is to obtain form-only functions of the smoothed state, its covariance and the tangent linear dynamical model, which can be effectively approximated through ensemble methods. To begin with, let us distinguish at iteration $l+1$ between the parameters to be sought, $(\boldsymbol{a}_{l+1}, \mathbf{Q}_{l+1})$, and the prior parameters, $(\boldsymbol{a}_l, \mathbf{Q}_l)$. After identifying that $\mathcal{Q}_1$ is independent of $(\boldsymbol{a}_{l+1}, \mathbf{Q}_{l+1})$, we can discard $\mathcal{Q}_1$ and focus on $\mathcal{Q}_2$ and $\mathcal{Q}_3$. By applying the expectation operator inside the sum operator[1] and using properties of the matrix trace (tr) (namely – for square matrices A and B – linearity: $tr(aA + bB) = atr(A) + btr(B)$, $tr(A^T) = tr(A)$ and $tr(X^TY) = tr(XY^T) = tr(Y^TX) = tr(YX^T), tr(X^TX) = \|X\|^2$, where X and Y are $n \times m$ matrices), $\mathcal{Q}_3$ can be expanded to first order as

$$\mathcal{Q}_3 = -\frac{K}{2} \ln |\mathbf{R}| - \frac{1}{2} \sum_{k=1}^{K} \Big(\|\mathbf{y}_k - \mathbb{H}(\mathbf{x}_{k|K})\|^2_{\mathbf{R}} + \mathrm{tr}\big[(\partial_{\mathbf{x}}\mathbb{H})^T \mathbf{R}^{-1} \partial_{\mathbf{x}}\mathbb{H}\, \mathbf{P}_{k|K}\big] \Big), \quad (19)$$

where K after the conditioning delimiter | is abbreviated notation for $\mathbf{y}_{1:K}$ and $\partial_{\mathbf{x}}\mathbb{H}$ denotes the tangent linear model of $\mathbb{H}$ around $\mathbf{x}_{k|K}$. The terms $\mathbf{x}_{k|K}$ and $\mathbf{P}_{k|K}$ denote the conditional mean and covariance of $\mathbf{x}_k$, respectively:

$$\mathbf{x}_{k|K} = \mathcal{E}_{\mathbf{x}_k|\mathbf{y}_{1:K}}(\mathbf{x}_k), \quad (20)$$

$$\mathbf{P}_{k|K} = \mathcal{E}_{\mathbf{x}_k|\mathbf{y}_{1:K}}(\mathbf{x}_k \mathbf{x}_k^T) - \mathbf{x}_{k|K} \mathbf{x}_{k|K}^T. \quad (21)$$

It can be easily verified that the terms $\mathbf{x}_{k|K}$ and $\mathbf{P}_{k|K}$ are independent of the parameter to be sought, $\boldsymbol{a}_{l+1}$; therefore $\mathcal{Q}_3$ does not depend on $\boldsymbol{a}_{l+1}$ (at first order) and can be discarded in the minimization. Similarly, applying the expectation operation inside the sum operator of $\mathcal{Q}_2$ gives

$$\mathcal{Q}_2 = -\frac{K-1}{2} \ln |\mathbf{Q}| - \frac{1}{2} \sum_{k=1}^{K} \Big(\|\mathbf{x}_{k|K} - \mathbf{x}^-_{k|K}\|^2_{\mathbf{Q}} + \mathrm{tr}\big[\mathbf{Q}^{-1}(\mathbf{P}_{k|K} + \mathbf{P}^-_{k|K} - \mathbf{P}^\dagger_{k|K} - (\mathbf{P}^\dagger_{k|K})^T)\big] \Big), \quad (22)$$

where we have defined the following:

$$\mathbf{x}^-_k = \varphi_k(\mathbf{x}_{k-1}, \boldsymbol{a}_{l+1}), \quad (23)$$

$$\mathbf{x}^-_{k|K} = \mathcal{E}_{\mathbf{x}_{k,k-1}|\mathbf{y}_{0:K}}(\varphi_k(\mathbf{x}_{k-1}, \boldsymbol{a}_{l+1})) \approx \varphi_k(\mathbf{x}_{k-1|K}, \boldsymbol{a}_{l+1}), \quad (24)$$

[1] We omit the prior θ_l in the expectation operator notation.

$$\mathbf{P}^{-}_{k|K} = \mathcal{E}_{\mathbf{x}_{k,k-1}|\mathbf{y}_{0:K}}\left((\mathbf{x}^{-}_{k} - \mathbf{x}^{-}_{k|K})(\mathbf{x}^{-}_{k} - \mathbf{x}^{-}_{k|K})^{T}\right)$$
$$= \mathcal{E}_{\mathbf{x}_{k,k-1}|\mathbf{y}_{0:K}}(\mathbf{x}^{-}_{k}\mathbf{x}^{-T}_{k}) - \mathbf{x}^{-}_{k|K}(\mathbf{x}^{-}_{k|K})^{T}, \quad (25)$$
$$\mathbf{P}^{\dagger}_{k|K} = \mathcal{E}_{\mathbf{x}_{k,k-1}|\mathbf{y}_{0:K}}\left((\mathbf{x}^{-}_{k} - \mathbf{x}^{-}_{k|K})(\mathbf{x}_{k} - \mathbf{x}_{k|K})^{T}\right)$$
$$= \mathcal{E}_{\mathbf{x}_{k,k-1}|\mathbf{y}_{0:K}}(\mathbf{x}^{-}_{k}\mathbf{x}^{T}_{k}) - \mathbf{x}^{-}_{k|K}\mathbf{x}^{T}_{k|K}, \quad (26)$$

where $\mathbf{x}^{-}_{k|K}$ and $\mathbf{P}^{-}_{k|K}$ are the conditional mean and covariance of $\mathbf{x}^{-}_{k}$, respectively. From now on, to simplify the notation, we will drop the dependences on $\mathbf{y}$ and $\mathbf{x}_{k,k-1}$ in the expectation. At first order, the term $\mathbf{P}^{-}_{k|K}$ can be rewritten in terms of the covariance $\mathbf{P}_{k-1|K}$:

$$\begin{aligned}\mathbf{P}^{-}_{k|K} &= \mathcal{E}_{\mathbf{x}}\{[\varphi_k(\mathbf{x}_{k-1}, \boldsymbol{a}_{l+1}) - \varphi_k(\mathbf{x}_{k-1|K}, \boldsymbol{a}_{l+1})]\\ &\quad [\varphi_k(\mathbf{x}_{k-1}, \boldsymbol{a}_{l+1}) - \varphi_k(\mathbf{x}_{k-1|K}, \boldsymbol{a}_{l+1})]^{T}\}\\ &= \mathcal{E}_{\mathbf{x}}\{\partial_{\mathbf{x}}\varphi_k(\mathbf{x}_{k-1|K}, \boldsymbol{a}_{l+1}) \cdot (\mathbf{x}_{k-1} - \mathbf{x}_{k-1|K})\\ &\quad (\mathbf{x}_{k-1} - \mathbf{x}_{k-1|K})^{T} \cdot \partial_{\mathbf{x}}\varphi^{T}_{k}(\mathbf{x}_{k-1|K}, \boldsymbol{a}_{l+1})\}\\ &= \partial_{\mathbf{x}}\varphi_k(\mathbf{x}_{k-1|K}, \boldsymbol{a}_{l+1}) \cdot \mathcal{E}_{\mathbf{x}}\{(\mathbf{x}_{k-1} - \mathbf{x}_{k-1|K})\\ &\quad (\mathbf{x}_{k-1} - \mathbf{x}_{k-1|K})^{T}\} \cdot \partial_{\mathbf{x}}\varphi^{T}_{k}(\mathbf{x}_{k-1|K}, \boldsymbol{a}_{l+1})\\ &= \partial_{\mathbf{x}}\varphi_k(\mathbf{x}_{k-1|K}, \boldsymbol{a}_{l+1})\mathbf{P}_{k-1|K}\partial_{\mathbf{x}}\varphi^{T}_{k}(\mathbf{x}_{k-1|K}, \boldsymbol{a}_{l+1}). \quad (27)\end{aligned}$$

In the second line above, we introduced the tangent linear operator of the model φ_k around $\mathbf{x}_{k-1|K}$ and its adjoint. These operators are denoted by $\partial_{\mathbf{x}}\varphi_k(\mathbf{x}_{k-1|K}, \boldsymbol{a})$ and $\partial_{\mathbf{x}}\varphi^{T}_{k}(\mathbf{x}_{k-1|K}, \boldsymbol{a})$, respectively. The same manipulations can be applied to the conditional cross-covariance of $\mathbf{x}_k$ and $\mathbf{x}^{-}_{k}$ denoted by $\mathbf{P}^{\dagger}_{k|K}$:

$$\begin{aligned}\mathbf{P}^{\dagger}_{k|K} &= \mathcal{E}_{\mathbf{x}}\{[\varphi_k(\mathbf{x}_{k-1}, \boldsymbol{a}_{l+1}) - \varphi_k(\mathbf{x}_{k-1|K}, \boldsymbol{a}_{l+1})](\mathbf{x}_{k} - \mathbf{x}_{k|K})^{T}\}\\ &= \mathcal{E}_{\mathbf{x}}\{\partial_{\mathbf{x}}\varphi_k(\mathbf{x}_{k-1|K}, \boldsymbol{a}_{l+1}) \cdot (\mathbf{x}_{k-1} - \mathbf{x}_{k-1|K})(\mathbf{x}_{k} - \mathbf{x}_{k|K})^{T}\}\\ &= \partial_{\mathbf{x}}\varphi_k(\mathbf{x}_{k-1|K}, \boldsymbol{a}_{l+1}) \cdot \mathcal{E}_{\mathbf{x}}\{(\mathbf{x}_{k-1} - \mathbf{x}_{k-1|K})(\mathbf{x}_{k} - \mathbf{x}_{k|K})^{T}\}. \quad (28)\end{aligned}$$

After these manipulations, we see that, when searching for $\boldsymbol{a}_{l+1}$, it is necessary to consider the covariance terms $\mathbf{P}^{-}_{k-1|K}$ and $\mathbf{P}^{\dagger}_{k|K}$ that are indeed both functions of $\boldsymbol{a}_{l+1}$. Indeed, this variance tensor parameter has a direct impact on the tangent linear operator $\partial_{\mathbf{x}}\varphi_k(\mathbf{x}_{k-1|K}, \boldsymbol{a}_{l+1})$. Note that if the dynamic model is linear, a closed form for $\boldsymbol{a}_{l+1}$ can be obtained by setting $\nabla_{\boldsymbol{a}}\mathcal{Q}_2 = 0$. Looking for $\mathbf{Q}_{l+1}$, the model error covariance, amounts to finding a $\mathbf{Q}_{l+1}$ solution of $\nabla_{\mathbf{Q}}\mathcal{Q}_2 = 0$. A closed-form solution generally exists regardless of the nature of the dynamics. However, as suggested in our stochastic formulation (Equation 8), $\boldsymbol{a}$ and $\mathbf{Q}$ are not entirely independent of each other. We therefore show in Section 5 a possible solution of this coupled problem within an ensemble assimilation framework for the physical parameter $\boldsymbol{a}$ as well as the model error covariance $\mathbf{Q}$.

4 | ENKF AND ENSEMBLE RTS SMOOTHER IN THE E-STEP

In the previous section, we showed that in the E-step a *smoothing* posterior distribution of the state conditioned on the whole data span and on the prior parameters must be found. The method for computing such a smoothing state is quite versatile. Methods referred to as the Rauch–Tung–Striebel (RTS) smoother, two-filter smoothing or joint smoothing enable us to perform such estimations. Interested readers may refer to Cosme *et al.* (2012) and the references therein for a complete review of these methods. In this study, we choose to rely on an ensemble version of the RTS smoother (EnRTS) similar to the one proposed in Raanes (2016), as this smoother can perform efficiently and is compatible with the ensemble Kalman filter (EnKF) methods.

4.1 | EnKF

The central idea underlying the EnKF consists in approximating the estimation covariance matrix with a few samples. Therefore, the intractable covariance evolution problem is transformed into a tractable sampling evolution followed by an empirical approximation. By denoting $\mathbf{E}_k$ as the ensemble state made up of N sampled states at time k,

$$\mathbf{E}_k = (\mathbf{x}_{1,k}, \dots, \mathbf{x}_{l,k}, \dots, \mathbf{x}_{N,k}) \in \mathbb{R}^{n \times N}, \quad (29)$$

the covariance can be approximated through the sampling covariance matrix $\mathbf{P}^{e}$:

$$\mathbf{P}_k \approx \mathbf{P}^{e} = \frac{1}{N-1}(\mathbf{E}_k - \overline{\mathbf{E}}_k)(\mathbf{E}_k - \overline{\mathbf{E}}_k)^{T}, \quad (30)$$

where the columns of $\overline{\mathbf{E}}_k$ consist of the ensemble mean, $\overline{\mathbf{x}}_k = \frac{1}{N}\sum_{l=1}^{N}\mathbf{x}_{l,k}$. It is also convenient to define the ensemble anomaly matrix $\mathbf{A}_k = (1/\sqrt{N-1})(\mathbf{E}_k - \bar{\mathbf{E}}_k)$ that leads to $\mathbf{P}_k = \mathbf{A}_k\mathbf{A}_k^{T}$. The forecast stage consists in propagating the posterior ensemble state $\mathbf{E}^{a}$ (called the *analysis* and denoted by superscript a) from previous time $k-1$ to current time k, yielding the prior ensemble state $\mathbf{E}^{f}$ (also referred to as the *forecast* ensemble):

$$\mathbf{E}^{f}_{k} = \varphi_k(\mathbf{E}^{a}_{k-1}). \quad (31)$$

The forecast covariance matrix is implicitly inferred from the forecast ensemble $\mathbf{P}^{f}_{k} = \mathbf{A}^{f}_{k}\mathbf{A}^{fT}_{k}$. The following analysis/update stage aims at estimating the correction of the state given the new observation $\mathbf{y}_k$ at time t_k. In the stochastic EnKF approach, an observation ensemble $\mathcal{Y}_k$ is built by perturbing the observation $\mathbf{y}_k$ with additive noise $\eta_l \propto \mathcal{N}(0, \mathbf{R})$. The update scheme reads

$$\mathbf{E}^{a}_{k} = \mathbf{E}^{f}_{k} + \mathbf{P}^{f}_{k}\partial^{T}_{\mathbf{x}}\mathbb{H}(\partial_{\mathbf{x}}\mathbb{H}\,\mathbf{P}^{f}_{k}\partial^{T}_{\mathbf{x}}\mathbb{H} + \mathbf{R})^{-1}(\mathcal{Y}_k - \mathbb{H}(\mathbf{E}^{f}_{k})). \quad (32)$$

In practice, $\mathbf{P}$ is never computed explicitly. An efficient implementation is formulated in terms of the ensemble anomaly matrix $\mathbf{A}$:

$$\mathbf{E}^{a}_{k} = \mathbf{E}^{f}_{k} + \mathbf{A}^{f}_{k}(\partial_{\mathbf{x}}\mathbb{H}\,\mathbf{A}^{f}_{k})^{T}\mathbf{S}^{-1}_{k}\mathbf{D}_k, \quad (33)$$

where we define $\mathbf{S}_k = \partial_{\mathbf{x}}\mathbb{H}\,\mathbf{A}^{f}_{k}(\partial_{\mathbf{x}}\mathbb{H}\,\mathbf{A}^{f}_{k})^{T} + \mathbf{R}$ and $\mathbf{D}_k = \mathcal{Y}_k - \mathbb{H}(\mathbf{E}^{f}_{k})$.

4.2 | EnRTS smoother

From a statistical perspective, a filtering problem seeks to estimate $\mathbf{x}_k$ by maximizing the posterior conditional

probability function $p(\mathbf{x}_k|\mathbf{y}_{0:k})$ given a sequence of past data up to the current time k. Smoothing, on the other hand, aims to estimate the posterior probability function $p(\mathbf{x}_k|\mathbf{y}_{0:K})$ conditioned on the whole data range from the initial time to the final time K. The filtering state ensemble $\mathbf{E}_{k|k}$ of EnKF serves as the input for the EnRTS smoother. Smoothing is performed recursively backward in time from the final time to the initial time. The smoothing ensemble state is given by

$$\mathbf{E}_{k|K} = \mathbf{E}^a_k + \mathbf{J}_k(\mathbf{E}_{k+1|K} - \varphi_k(\mathbf{E}^a_k)), \tag{34}$$

with $\mathbf{E}_{K|K} = \mathbf{E}^a_K$. In Equation 34, $\mathbf{J}_k$ reads as (eq. 17 in Raanes, 2016)

$$\mathbf{J}_k = \mathbf{A}^a_k(\mathbf{A}^f_{k+1})^+, \tag{35}$$

where the superscript + stands for the Moore–Penrose inverse that can be computed through the singular value decomposition (SVD) given that the ensemble approximated covariance is of reduced rank. This formulation can therefore be applied directly to the ensemble anomaly matrix as long as the forecast/analysis ensembles supplied by the EnKF are stored in memory. Note that the ensemble Kalman smoother (EnKS) is also a viable choice for producing the smoothing state. Interested readers may refer to Raanes (2016) for a comparative study of the EnRTS smoother and the EnKS.

4.3 | Localization in the EnKF and EnRTS smoother

The standard localization schemes must be applied to the EnKF scheme to handle the unavoidable fictitious long-range correlations emerging in low-rank sampled correlation matrices of a high-dimensional system. In this paper, we extend the Schur product-based covariance localization scheme to the EnRTS smoother. In this approach, we use an altered form of the global ensemble sampling matrix to compute $\mathbf{J}_k$:

$$\mathbf{J}_k = \mathcal{A}^a_k(\mathcal{A}^f_{k+1})^{-1}, \tag{36}$$

where $\mathcal{A}$ is a localized version of $\mathbf{A}$ such that $\mathcal{A}\mathcal{A}^T = \mathbf{L} \odot (\mathbf{A}\mathbf{A}^T)$. Therefore, the EnRTS smoother update scheme with a localized covariance stays in exactly the same form. It remains just to replace $\mathbf{A}$ by its localized counterpart $\mathcal{A}$.

5 | AN ENSEMBLE FORMULATION OF THE M-STEP

In the previous section, we introduced the EnKF and the EnRTS smoother to solve the E-step at the $(l+1)$th EM iteration. The ensemble E-step yields the smoothing ensemble state $\mathbf{E}_{k|K}$. A low-rank approximation of the smoothing covariance $\mathbf{P}_{k|K}$ as well as $\mathbf{P}^-_{k|K}$ and $\mathbf{P}^\dagger_{k|K}$ in Equation 22 are provided by the smoothing ensemble anomaly matrix $\mathbf{A}_{k|K}$:

$$\mathbf{x}_{k|K} = \overline{\mathbf{E}}_{k|K}, \tag{37}$$

$$\mathbf{P}_{k|K} = \mathbf{A}_{k|K}\mathbf{A}^T_{k|K}, \tag{38}$$

$$\mathbf{P}^-_{k|K} = \mathbf{A}^-_{k|K}(\boldsymbol{a}_{l+1})(\mathbf{A}^-_{k|K}(\boldsymbol{a}_{l+1}))^T, \tag{39}$$

$$\mathbf{P}^\dagger_{k-1,k|K} = \mathbf{A}^-_{k|K}(\boldsymbol{a}_{l+1})\mathbf{A}^T_{k|K}, \tag{40}$$

where $\mathbf{A}^-_{k|K}(\boldsymbol{a}_{l+1})$ denotes the evolution of the smoothing ensemble anomaly matrix $\mathbf{A}_{k-1|K}$, expressed as the difference between the smoothing ensemble driven by the nonlinear model and its mean:

$$\begin{aligned}\mathbf{A}^-_{k|K}(\boldsymbol{a}_{l+1}) &\triangleq \partial_{\mathbf{x}}\varphi_k(\mathbf{x}_{k-1|K})\mathbf{A}_{k-1|K} \\ &\approx \frac{1}{\sqrt{N-1}}\Big(\varphi_k(\mathbf{E}_{k-1|K}) - \varphi_k(\overline{\mathbf{E}}_{k-1|K})\Big).\end{aligned} \tag{41}$$

Substituting the above ensemble approximations into Equation 22 and defining the cost function $J^M = -Q_2$ allows us to transform the maximization problem into a minimization one with

$$\begin{aligned}J^M(\boldsymbol{a}_{l+1}, \mathbf{Q}_{l+1}) &= \frac{K-1}{2}\ln|\mathbf{Q}_{l+1}| \\ &+ \frac{1}{2}\sum_{k=1}^{K}\Big(\big\|\mathbf{x}^-_{k|K}(\boldsymbol{a}_{l+1}) - \mathbf{x}_{k|K}\big\|^2_{\mathbf{Q}_{l+1}} \\ &+ \mathrm{tr}\big[(\mathbf{A}^-_{k|K}(\boldsymbol{a}_{l+1}) - \mathbf{A}_{k|K})^T\mathbf{Q}^{-1}_{l+1}(\mathbf{A}^-_{k|K}(\boldsymbol{a}_{l+1}) - \mathbf{A}_{k|K})\big]\Big).\end{aligned} \tag{42}$$

We make the following remarks on Equation 42:

- In our stochastic dynamics (Equation 8), the random part depends on $\boldsymbol{a}$; therefore, minimizing J^M directly against $\boldsymbol{a}$ requires computing $\partial\mathbf{Q}/\partial\boldsymbol{a}$. This can be computationally demanding for a high-dimensional state and parameters. As a result, we employ a decoupled estimation procedure in which J^M is minimized with respect to $\boldsymbol{a}$ using the current estimate $\mathbf{Q}$ (which can be factored and hence plays only an indirect role in the minimization through the ensemble driven by the random dynamics and the Q-Wiener process; see Section 5.1). The minimization of J^M is then led with respect to $\mathbf{Q}$, with J^M evaluated using the current estimate $\boldsymbol{a}_{l+1}$ (Section 5.2).

5.1 | Physical stochastic parameter estimation

To facilitate the ensemble formulation, the cost function (42) may be reformulated (at first order) in terms of the increment $\delta\boldsymbol{a}_{l+1} \triangleq \boldsymbol{a}_{l+1} - \boldsymbol{a}_l$:

$$\begin{aligned}J^M(\delta\boldsymbol{a}_{l+1}) = \frac{1}{2}\sum_{k=1}^{K}\Bigg\{\sum_{j=1}^{N}\Bigg\|\Bigg\{\frac{1}{\sqrt{N-1}}\big[\varphi_k(\mathbf{E}_{k-1|K}, \boldsymbol{a}_l) \\ - \varphi_k(\overline{\mathbf{E}}_{k-1|K}, \boldsymbol{a}_l) + \big(\partial_{\boldsymbol{a}}\varphi_k(\mathbf{E}_{k-1|K}, \boldsymbol{a}_l) \\ - \partial_{\boldsymbol{a}}\varphi_k(\overline{\mathbf{E}}_{k-1|K}, \boldsymbol{a}_l)\big)\delta\boldsymbol{a}_{l+1}\big] - \mathbf{A}_{k|K}\Bigg\}_j\Bigg\|^2_{\mathbf{Q}} \\ + \Big\|\varphi_k(\mathbf{x}_{k-1|K}, \boldsymbol{a}_l) - \mathbf{x}_{k|K} + \partial_{\boldsymbol{a}}\varphi_k(\mathbf{x}_{k-1|K}, \boldsymbol{a}_l)\delta\boldsymbol{a}_{l+1}\Big\|^2_{\mathbf{Q}}\Bigg\},\end{aligned} \tag{43}$$

where the first term on the right-hand side of Equation 42 is discarded as it depends only on $\mathbf{Q}$, and the term $\partial_{\boldsymbol{a}}\varphi_k(\mathbf{x}_{k-1|K}, \boldsymbol{a}_l)$ denotes the tangent linear model of φ_k with

respect to $\boldsymbol{a}$:

$$\lim_{\alpha\to 0}\frac{\varphi_k(\mathbf{x}_k,\boldsymbol{a}+\alpha d\boldsymbol{a})-\varphi_k(\mathbf{x}_k,\boldsymbol{a})}{\alpha}=\partial_{\boldsymbol{a}}\varphi_k(\mathbf{x}_k,\boldsymbol{a})d\boldsymbol{a}. \tag{44}$$

In the same spirit as the ensemble methods, where the increment is sought in the range of the ensemble anomaly matrix, we introduce here an additional ensemble induced by the perturbation of $\boldsymbol{a}$. Such a perturbation gives rise to an ensemble $\mathbf{E}_{\boldsymbol{a}}\in\mathbb{R}^{p\times M}$, where p is the size of the parameter vector and M is the size of the parameter ensemble. In doing so, we fix the search space in the span of the column vectors of $\mathbf{A}_{\boldsymbol{a}}$:

$$\delta\boldsymbol{a}_{l+1}=\mathbf{A}_{\boldsymbol{a}}\Upsilon=\frac{1}{\sqrt{N-1}}(\mathbf{E}_{\boldsymbol{a}}-\bar{\mathbf{E}}_{\boldsymbol{a}})\Upsilon. \tag{45}$$

The cost function in terms of Υ now reads

$$\begin{aligned}J^M(\Upsilon)=\frac{1}{2}\sum_{k=1}^{K}\Bigg\{\sum_{j=1}^{N}\Bigg\|\Big\{\frac{1}{\sqrt{N-1}}[\varphi_k(\mathbf{E}_{k-1|K},\boldsymbol{a}_l)\\ -\varphi_k(\overline{\mathbf{E}}_{k-1|K},\boldsymbol{a}_l)]-\mathbf{A}_{k|K}+\frac{1}{N-1}\big(\partial_{\boldsymbol{a}}\varphi_k(\mathbf{E}_{k-1|K},\boldsymbol{a}_l)\\ -\partial_{\boldsymbol{a}}\varphi_k(\overline{\mathbf{E}}_{k-1|K},\boldsymbol{a}_l)\big)\mathbf{A}_{\boldsymbol{a}}\Upsilon\Big\}\Bigg\|_{\mathbf{Q}}^2\\ +\Bigg\|\varphi_k(\mathbf{x}_{k-1|K},\boldsymbol{a}_l)-\mathbf{x}_{k|K}\\ +\frac{1}{\sqrt{N-1}}\partial_{\boldsymbol{a}}\varphi_k(\mathbf{x}_{k-1|K},\boldsymbol{a}_l)\mathbf{A}_{\boldsymbol{a}}\Upsilon\Bigg\|_{\mathbf{Q}}^2\Bigg\}.\end{aligned} \tag{46}$$

The terms $\partial_{\boldsymbol{a}}\varphi_k(\mathbf{x}_{k-1|K},\boldsymbol{a}_l)\mathbf{A}_{\boldsymbol{a}}$ and $\partial_{\boldsymbol{a}}\varphi_k(\overline{\mathbf{E}}_{k-1|K},\boldsymbol{a}_l)\mathbf{A}_{\boldsymbol{a}}$ denote the evolution of the parameter ensemble perturbation through the tangent linear model with respect to the smoothed state $\mathbf{x}_{k-1|K}$. These two terms can be approximated in a similar way as in Equation 41. The tricky part is computing $\partial_{\boldsymbol{a}}\varphi_k(\mathbf{E}_{k-1|K},\boldsymbol{a}_l)\mathbf{A}_{\boldsymbol{a}}$, since the tangent linear term $\partial_{\boldsymbol{a}}\varphi_k(\mathbf{E}_{k-1|K},\boldsymbol{a}_l)$ is a function of the state ensemble. Therefore, evaluating this term involves perturbing each state sample with the parameter ensemble

$$\begin{aligned}&\partial_{\boldsymbol{a}}\varphi_k(\mathbf{E}_{k-1|K},\boldsymbol{a}_l)(\mathbf{E}_{\boldsymbol{a}}-\bar{\mathbf{E}}_{\boldsymbol{a}})\\ &\approx\big[\varphi_k(\mathbf{x}^1_{k-1|K},\mathbf{E}_{\boldsymbol{a}})-\varphi_k(\mathbf{x}^1_{k-1|K},\overline{\mathbf{E}}_{\boldsymbol{a}}),\dots,\\ &\quad\varphi_k(\mathbf{x}^N_{k-1|K},\mathbf{E}_{\boldsymbol{a}})-\varphi_k(\mathbf{x}^N_{k-1|K},\overline{\mathbf{E}}_{\boldsymbol{a}})\big].\end{aligned} \tag{47}$$

Here $\varphi_k(\mathbf{x}^j_{k-1|K},\mathbf{E}_{\boldsymbol{a}})\in\mathbb{R}^{n\times M}$, as φ_k is applied to $\mathbf{x}^j_{k-1|K}$ and each column of $\mathbf{E}_{\boldsymbol{a}}$. The above ensemble approximation yields an ensemble of ensembles with $N\times M$ state samples in total. Although the computational time needed for simulating the whole sample space trajectory is potentially larger, the ensemble implementation itself is simple and its high parallelism potential has not been weakened. Parallelization techniques can thus be introduced to reduce the computing time. Besides, memory space can be saved because we do not need to store all time series of the ensemble of $N\times M$ members as long as their contributions to the corresponding cost function term are computed and accumulated. Finally, all terms in Equation 46 can be derived from the smoothing state ensemble $\mathbf{E}_{k|K}$ and the parameter ensemble $\mathbf{E}_{\boldsymbol{a}}$. The ensemble approximation transforms the original nonlinear least-squares optimization problem to a (Gauss–Newton-like) series of incremental linear systems (in terms of the anomaly ensemble coefficients Υ) that can be solved efficiently using a gradient-based algorithm such as the conjugate gradient method.

5.2 | Model error covariance estimation

In the general case, the model error covariance term $\mathbf{Q}$ can be optimally estimated by simply setting to zero the derivative of formula $\mathcal{Q}_2$ (Equation 22) with respect to $\mathbf{Q}$. At the lth M-step in the EM iteration, the re-estimated $\mathcal{Q}$ reads as

$$\begin{aligned}\mathbf{Q}_{l+1}=&\frac{1}{K-1}\sum_{k=1}^{K}[\mathcal{E}_{\mathbf{x}}(\mathbf{x}_k\mathbf{x}_k^T)+\mathcal{E}_{\mathbf{x}}(\mathbf{x}_k^-\mathbf{x}_k^{-T})\\ &-\mathcal{E}_{\mathbf{x}}(\mathbf{x}_k^-\mathbf{x}_k^T)-\mathcal{E}_{\mathbf{x}}(\mathbf{x}_k(\mathbf{x}_k^-)^T)].\end{aligned} \tag{48}$$

Using similar ensemble formulations, we derive the following scheme in evaluating $\mathbf{Q}$:

$$\begin{aligned}\mathbf{Q}_{l+1}=&\frac{1}{K-1}\sum_{k=1}^{K}\Big([\mathbf{A}^-_{k|K}(\boldsymbol{a}_{l+1})-\mathbf{A}_{k|K}][\mathbf{A}^-_{k|K}(\boldsymbol{a}_{l+1})-\mathbf{A}_{k|K}]^T\\ &+[\mathbf{x}^-_{k|K}(\boldsymbol{a}_{l+1})-\mathbf{x}_{k|K}][\mathbf{x}^-_{k|K}(\boldsymbol{a}_{l+1})-\mathbf{x}_{k|K}]^T\Big).\end{aligned} \tag{49}$$

Note that $\mathbf{A}^-_{k|K}$ and $\mathbf{x}^-_{k|K}$ have to be recomputed using the re-estimated parameters $\boldsymbol{a}_{l+1}$ at the lth EM iteration. We summarize the steps of the proposed ensemble-based EM algorithm below.

Algorithm 1 Ensemble-based EM algorithm

1: Given an observation sequence $\mathbf{y}$ from 0 to K, a prior initial state $\mathbf{x}_l^0$ and prior parameters $\boldsymbol{a}_l$ and $\mathbf{Q}_l$ at $l=0$:
2: **while** the convergence criterion is not met **do**
3: **Expectation step:**
4: **for** $k=0:K$ **do**
5: Forecasting state ensemble update (Equation 31) with parameter $\boldsymbol{a}_l$ and additive error resampled from $\mathbf{Q}_l$ using SVD
6: Filtering state ensemble update (Equation 33)
7: **end for**
8: Smoothing state ensemble update (Equation 34)
9: **Maximization step:**
10: Obtain $\boldsymbol{a}_{l+1}$ through Equation 46 and recover $\delta\boldsymbol{a}_{l+1}$ using Equation 45
11: Update model error covariance $\mathbf{Q}_{l+1}$ using Equation 49
12: Set $l\doteq l+1$, $\boldsymbol{a}_l\doteq\boldsymbol{a}_{l+1}$ and $\mathbf{Q}_l\doteq\mathbf{Q}_{l+1}$, then return to step 2.
13: **end while**

Let us outline how the noise resampling procedure requires some care. The noise sampling can be performed through two additive noises with diffusion matrices associated with the square roots $\mathbf{A}^-_{k|K}-\mathbf{A}_{k|K}$ and $\mathbf{x}^-_{k|K}-\mathbf{x}_{k|K}$, respectively. However,

these noises must be kept independent (in order to obtain the right covariance). To do this, the eigenspace of the first covariance matrix can be split into two complementary subspaces in order to sample the two independent noises. The first one is used to sample the first noise while a projection on the complementary subspace is used to sample the second one. Note that the first square root is likely to have a greater number of non-zero singular values as it relies on the ensemble of ensembles, as opposed to the second one which is associated with the ensemble of trajectories.

6 | DISCUSSIONS

In this section, we present a detailed discussion on the comparison between the proposed EM-based parameter estimation scheme and other prominent methods in the literature.

6.1 | Differences compared to Dreano *et al.* (2017) and Pulido *et al.* (2018)

Dreano *et al.* (2017) proposed an EM-based technique for estimating the model error covariance $\mathbf{Q}$, followed by a resampling of the model error $\boldsymbol{\xi}_k$ from the current covariance $\mathbf{Q}_{l+1}$ to simulate the optimal state trajectories. In their set-up the estimation of $\mathbf{Q}$ has a closed-form formulation based on an ensemble approximation (eqs. 18 and 44 in Dreano *et al.*, 2017). This formulation corresponds only to the second line of Equation 49 and can be interpreted as a first-order approximation of our complete formulation (Equation 49). Besides, our formulation for $\mathbf{Q}_{l+1}$ requires the re-estimation of the physical parameters $\boldsymbol{a}$ beforehand. For complex error terms, such as parametric error or multiplicative error, their approach may alter the error characterization by estimating an additive Gaussian error covariance that compensates for the error. Pulido *et al.* (2018) used the same EM algorithm as Dreano *et al.* (2017) for evaluating the model error covariance. They restated the limitation of the EM algorithm when dealing with physical parameters, as closed analytical forms for estimating the physical parameters generally do not exist. So, as an alternative mean to estimate the physical parameters with an EM technique, Pulido *et al.* (2018) proposed relying on an augmented state technique, in which the state and the parameter are jointly estimated during the filtering/smoothing phase of the E-step, whereas the augmented model error covariance is estimated in the M-step. This approach is shown to perform well in terms of the one-scale Lorenz-96 system with a specific polynomial noise term whose coefficients are defined from a Gaussian process. In this way, the mean and the variance of the corresponding component, acting as the deterministic parameter and the stochastic parameter, respectively, can both be estimated using the E-step and the M-step of this augmented state EM technique. Nevertheless, the particular form of the model limits any generalizations of their approach. We note that this approach has the same restriction in terms of the parameter dimension as the augmented state technique and has been used to estimate only parameters of very small dimension. Contrary to these strategies, our formulation is able to identify not only the unknown parameters, associated with any forms of the dynamics, but also the model error covariance. We will show in the experimental section that it is also beneficial to use a full EM algorithm to estimate physical parameters of much higher dimensions.

Apart from the EM approach based on the augmented state technique, Pulido *et al.* (2018) also resorted to a maximum likelihood (ML) approach that seeks to maximize the likelihood function of the observations given the parameters $p(\mathbf{y}_{1:K}|\boldsymbol{\theta})$. Their formulation, relying on the Markov property of time-sequential data and the Bayes rule, led to the factorized form

$$\ln p(\mathbf{y}_{1:K}|\boldsymbol{\theta}) = \ln \prod_{k=1}^{K} p(\mathbf{y}_k|\mathbf{y}_{1:k-1}, \boldsymbol{\theta}). \tag{50}$$

For comparison purposes, we recall here the marginalized full joint distribution over the state $\mathbf{x}$ used in the EM algorithm:

$$\ln p(\mathbf{y}_{1:K}|\boldsymbol{\theta}) = \ln \sum_{\mathbf{x}} p(\mathbf{y}_{1:K}, \mathbf{x}_{0:K}|\boldsymbol{\theta}). \tag{51}$$

One advantage of the ML approach is that only the filter is required to obtain a solution. By introducing the state-space formulation (Equations 10–12) to $p(\mathbf{y}_k|\mathbf{y}_{1:k-1}, \boldsymbol{\theta})$, the Kalman filter solution is exactly recovered for linear models and additive Gaussian errors. For general nonlinear and/or non-Gaussian cases, Monte Carlo methods must be employed to approximate this distribution. The challenge in terms of the formulation (Equation 50) is that, in the case of non-additive model error, the gradient of the likelihood w.r.t. $\boldsymbol{\theta}$ can be hard to evaluate. To that end, Pulido *et al.* (2018) proposed a derivative-free optimization method to maximize $\ln p(\mathbf{y}_{1:K}|\boldsymbol{\theta})$. However, despite their practical interest, derivative-free methods are generally not among the most efficient optimization techniques. The original likelihood form (Equation 51) in EM is, on the other hand, hard to manipulate, so a lower bound that is iteratively increased towards the original likelihood (Equation 51) is defined instead. A great advantage of EM, as compared to the ML approach, is that in order to maximize $\mathcal{Q}$ (Equation 13) in the M-step, only the complete joint distribution of the state and the observation conditioned on the parameters is needed, since the posterior conditional distribution term is known from the E-step. Indeed, in many scenarios, deriving the gradient of the complete joint distribution w.r.t. the parameters is much easier than deriving the gradient of Equation 50.

6.2 | Differences compared to the dual Kalman filter approach

Delsole and Yang (2010) advocated the use of a generalized ML approach to estimate the model state and the stochastic parameters. This approach is still based on the

maximization of the posterior *joint* conditional distribution $p(\mathbf{x}, \boldsymbol{\theta}|\mathbf{y})$. Instead of using an augmented state technique, however, which can cause ensemble collapsing, the optimization process is decoupled into two alternate procedures, in which the parameters and the state are alternately optimized. The procedure can be implemented through two separated Kalman-like filters, namely a state filter and a parameter filter. This approach is an online method. Such a dual filter technique can be readily extended to the dual ensemble filter approach to handle nonlinear dynamical operators.

Compared to this technique, our (offline) EM-based approach maximizes the marginalized complete joint distribution through an alternate optimization. In addition, it provides a coupled estimation of the smoothed state $\mathbf{x}_{0:K}$ and of the parameter $\boldsymbol{\theta}$ given the set of observations from 0 to K.

Another major difference concerns the treatment of the error covariance term (denoted as $\mathbf{P}^f$ in Delsole and Yang (2010) and $\mathbf{Q}$ in our manuscript). Note that $\mathbf{P}^f$ in a filter context corresponds to the composition of the background error covariance's evolution $\mathbf{P}_0$ and of the model error covariance $\mathbf{Q}$. The filtering formulations in Delsole and Yang (2010) are general, so they can be applied to deterministic or stochastic parameter estimation problems. However, the authors focus on a particular case where the error covariance is a function of the stochastic parameter. The formula for updating the parameters in the parameter–filter stage requires the derivative w.r.t. the parameters of the covariance term $\mathbf{P}^f$. Due to the complexity of computing these derivatives, the authors proposed an evaluation technique relying on an additional parameter-induced ensemble, in the same way as we did. Formally in our stochastic shallow-water model, the variance tensor $\boldsymbol{a}$ plays a role both in the drift part and in the random part. The random term is a non-Gaussian error term that cannot easily be estimated directly. We thus first estimate the variance tensor $\boldsymbol{a}$ as a deterministic physical parameter accompanied by a centred Gaussian error of covariance $\mathbf{Q}$, then, as depicted in Algorithm 1, we consider a decoupled estimation approach by minimizing the cost function $\mathcal{Q}_2$ (Equation 22) w.r.t. $\boldsymbol{a}$ and $\mathbf{Q}$ separately in the M-step.

Apart from the fundamental differences discussed above, our formulation thus shares similarities with Delsole and Yang (2010) in the way that the gradient of the state w.r.t. the parameters is approximated using an ensemble of ensembles.

6.3 | Differences compared to Ueno and Nakamura (2014)

Ueno and Nakamura (2014) proposed estimating the observation error covariance $\mathbf{R}$ in an ML framework, and they exploited the equivalent formulation between the sampling-based likelihood function and the Gaussian mixture model. Based on this link, the authors employed the EM algorithm to iteratively estimate $\mathbf{R}$ and the latent mixture components. For comparison purposes, we show here the estimation of $\mathbf{R}$ that ensues from our approach and the maximization of the $\mathcal{Q}_3$ term (Equation 18). By solving $\nabla_{\mathbf{R}}\mathcal{Q}_3 = 0$ with the ensemble approximation, we get

$$\mathbf{R}_{l+1} = \frac{1}{K}\sum_{k=1}^{K}[\|\mathbf{y}_k - \mathbb{H}(\mathbf{x}_{k|K})\|^2 + \partial_{\mathbf{x}}\mathbb{H}\,\mathbf{A}_{k|K}(\partial_{\mathbf{x}}\mathbb{H}\,\mathbf{A}_{k|K})^T], \tag{52}$$

which can be computed using the smoothed ensemble state. Comparing this expression with formula 35 in Ueno and Nakamura (2014), we observe that the EM approach in Ueno and Nakamura (2014) does not involve any state inference problem in the E-step, as their updating formula 35 corresponds only to an innovation term (i.e., the first term of eq. 48) related to the filtered state. Their approach thus requires only an EnKF procedure before proceeding to the EM algorithm. Due to this trait, their method can be implemented online. However, it cannot be used to estimate the state and the model error covariance $\mathbf{Q}$. This approach has been extended in Ueno and Nakamura (2016) to incorporate a prior model on $\mathbf{R}$ and to proceed to a Bayesian a posteriori estimation.

7 | ENVAR-EM WITH AUGMENTED STATE

An alternative approach consists in combining the EM algorithm with EnVar (Yang and Mémin, 2017) to estimate the parameters using an augmented state technique. The iterative procedure in EM is in the same spirit as the iterative resampling strategy used in the EnVar technique proposed in Yang *et al.* (2015). This technique, built from a Gauss–Newton nested-loop variational framework, contains an update step of both the prior/posterior ensemble and the associated ensemble anomaly matrix. The cost function (in non-incremental form) in terms of the augmented state vector $\mathbf{s}_k = [\mathbf{x}_k, \boldsymbol{a}]^T$ reads as

$$J(\mathbf{s}_0) = \frac{1}{2}\|\mathbf{s}_0\|^2_{\mathbf{B}^f_{\mathbf{s}}} + \frac{1}{2}\sum_{k=0}^{K}\|\mathbb{H}(\varphi_k(\mathbf{s}_0)) - \mathbf{y}_k\|^2_{\mathbf{R}}, \tag{53}$$

where the augmented error covariance matrix $\mathbf{B}_{\mathbf{s}}$ is given by

$$\begin{pmatrix} \mathbf{B}_{xx} & \mathbf{B}^T_{ax} \\ \mathbf{B}_{ax} & \mathbf{B}_{aa} \end{pmatrix}. \tag{54}$$

Note that the EnVar method relies on a strong dynamical constraint, thus no explicit model error term is considered here. However, between two consecutive outer loops, the covariance matrix $\mathbf{B}_{aa}$ along with $\mathbf{B}_{\mathbf{xx}}$ is re-estimated following the joint update of the augmented state/parameter vector. This strategy, which is similar to the one used in Pulido *et al.* (2018), can be interpreted as the *maximization* step in the EM algorithm. For the experimental assessments presented in the next section, we applied both the Aug-EnVar-EM method and the proposed EnKF/EnRTS-EM method to the same dynamical models and datasets. The goal here is to evaluate numerically the behaviour differences between the augmented state techniques and the EM algorithm in retrieving unknown state/parameter fields.

8 | EXPERIMENTS AND RESULTS

8.1 | Experimental settings

We devised two different scenarios using a similar experimental set-up as in Yang and Mémin (2017). In all cases, we use the one-dimensional stochastic shallow-water system (Equation 8). The one-dimensional domain has length $L_x = 6,000$ km with the initial surface height $h(x, 0)$ given by

$$h(x,0) = H_0 - \frac{fU_0 x}{g} + A\xi(x), \tag{55}$$

where $H_0 = 5,000\,\mathrm{m}$, $f = 1.03 \times 10^{-4}\mathrm{s}^{-1}$ is the Coriolis parameter, $U_0 = 40\,\mathrm{m/s}$ and g is the gravity acceleration. An additional noise is considered for the initial condition with $A = 10$ as its amplitude. The Gaussian random field ξ is simulated through the spectral method discussed in Evensen (2003) (with a de-correlation length equal to $20\%L_x$). The initial velocity field is inferred from the geostrophic relation.

The first case corresponds to a typical state and parameter estimation problem, for which the true stochastic parameter distribution is known. The background state is run on the same resolution (26 grid points) as the true state simulation. The objective of this case is to evaluate quantitatively the performance of different approaches in the recovery of the parameters as well as the state.

Case II corresponds to the same configurations as those used in Yang and Mémin (2017), where no true model of the parameters is prescribed. Instead, the resolution-induced error is intrinsically defined and parameterized according to the stochastic dynamics. In that case, the quality of the estimated parameters can only be implicitly evaluated through the accuracy of the state recovery. To that end, the coarse-resolution background state with the same initial condition as in Case I is simulated with the stochastic model on 26 grid points, while the true state used to construct the fine-resolution observation is obtained by integrating the standard shallow-water equation with the initial condition (Equation 55) on a grid of finer resolution (401 grid points). Meanwhile, the time step Δt is set to 15 s for the true state model and to 30 s for the coarse-resolution model in order to satisfy the different Courant-Friedrichs-Lewy (CFL) conditions.

In both cases, the synthetic observations are extracted from the true state every 150 s by adding an i.i.d. Gaussian noise to the true state. The magnitude of the noise level is proportional to the background errors.

The EnKF and the EnRTS smoother are used to produce the optimal state estimation given the observations. The parameter estimation resulting from the EM algorithm is compared with the Aug-EnVar-EM approach, implementing an augmented state technique. In all ensemble-related computations, we have used 32 members combined with a covariance localization technique based on a Schur product with the Gaspari–Cohn kernel (Gaspari and Cohn, 1999) (see Section 4.3).

8.2 | Case I: EM numerical assessment with known true parameter

In this first case, we try to recover both the noisy background state and the unknown parameter field. Because the true parameter field is invariant in time, a single assimilation window containing all five observations is employed for the augmented EnVar approach. As the EnKF/EnRTS smoother is sequentially implemented, the five observations are successively assimilated. The analysis is started at time $t = 600$ s to maintain the balance of the state variables in the ensemble.

Depending on our EM algorithm formulation, whether or not the M-step can find the optimal parameter hinges on the quality of the posterior state given by the E-step. In Figure 1, we plot Root-mean-square Error (RMSE) curves of different posterior states (h and u for the top and bottom figures, respectively) after consecutive EnKF/EnRTS-EM iterations. It can be observed that, immediately after the first E-step, the smoothed state at each observational time is already of excellent quality. The subsequent iterations improve progressively further the results in making the RMSE curves flatter. The flatness of the analysis RMSE curves reflects the accuracy of the estimated variance tensor parameter.

To examine the effectiveness of the maximization step of EnKF/EnRTS-EM, we begin by plotting the RMSE of the posterior parameter with respect to the reference true parameter against 10 EM iterations in Figure 2. In the current scenario, the RMSE result indicates that the EnKF/EnRTS-EM converges fairly fast in three iterations.

In the left column of Figure 3, we plot the exact spatial forms of the estimated posterior parameter field (dotted line) yielded at each EM iteration along with the current prior parameter (dashed line), the background parameter (solid line) and the reference true parameter (dash-dotted line) in terms of EM iterations. Note that at the first iteration, the prior parameter is equal to the background parameter. We can verify that the true parameter field is successfully recovered by EnKF/EnRTS-EM after the third iteration, although the fourth and fifth iterations continue to improve the accuracy of the posterior parameter. The right column of Figure 3 depicts the evolution of the posterior parameter using Aug-EnVar-EM in terms of the outer loop iteration. The parameter evolution converges after the third iteration as well. Nevertheless, the sought parameter field only partly coincides with the true parameter field. In terms of the accuracy of the estimated parameter, the EnKF/EnRTS-EM method greatly outperforms Aug-EnVar-EM.

Finally, we compare the state RMSE after the final E-step of EnKF/EnRTS-EM and Aug-EnVar-EM in Figure 4. Compared to the smoothed trajectory provided by EnKF/EnRTS-EM, the initial analysis state of Aug-EnVar-EM is more accurate. However the inaccuracy of the parameter estimation eventually interferes with the dynamics and causes the trajectory to diverge from the reference trajectory, leading to a bad forecast. This is a typical

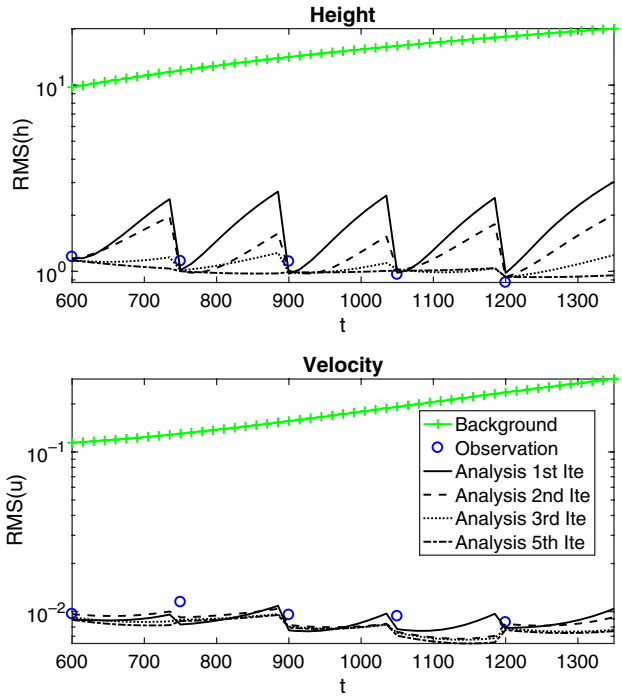

FIGURE 1 Case I: comparison of state Root-mean-square Error (RMSE) evolution for EnKF/EnRTS-EM. Solid, dashed, dotted and dash-dotted lines denote the analysis trajectory yielded after the first, second, third and fifth E-step iterations, respectively, from a total of 10 iterations [Colour figure can be viewed at wileyonlinelibrary.com]

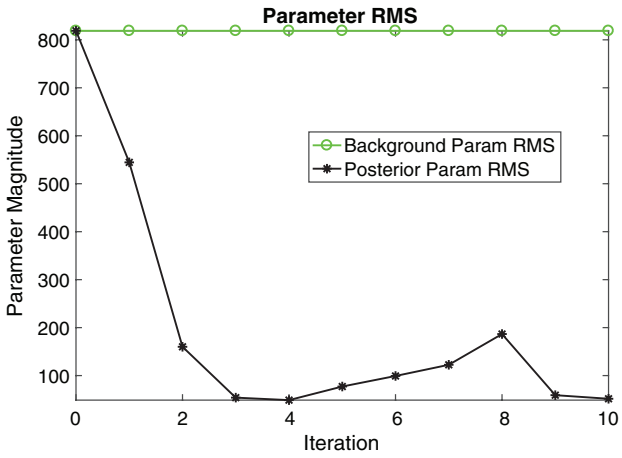

FIGURE 2 Case I: parameter RMSE against EnKF/EnRTS-EM iterations [Colour figure can be viewed at wileyonlinelibrary.com]

example of the overfitting phenomenon. The analysis state yielded by Aug-EnVar-EM corresponds too closely to the observations, but the parameters estimated from the augmented state approach, even combined with the EM strategy, lead to large generalization errors, resulting in bad predictive performance of the trained model.

8.3 | Case II: EM numerical assessment with unknown parameter

Finally, we tested different parameter estimation approaches for minimizing the errors due to scale discrepancy. Since the variance tensor $\boldsymbol{a}$ to be sought is time varying, it is necessary to introduce a sliding assimilation window technique, in which the parameters are assumed invariant during one window and are then allowed to vary when shifted to the next window. For the Aug-EnVar-EM approach, we employed three cycling windows for six observations. We also considered an extreme case where one window only contains one observation and the analysis time is set to the observation time. In that case, the Aug-EnVar-EM reduces to the Aug-EnKF-EM.

A similar sliding window technique was also applied to the EnKF/EnRTS-EM approach to incorporate the fast-changing variance tensor. Here we implemented an adapted version of the offline ensemble-based EM scheme shown in Algorithm 1. In the original algorithm, the parameters were kept invariant during the full observation sequence from $\mathbf{y}_0$ to $\mathbf{y}_K$. In the adapted version, we introduced K sub-windows. Each sub-window started from the first observation and proceeded through successive $(K-1)$th observations before ending at the final Kth observation. In doing so, we are able to update the variance tensors when a new observation occurs but also to take account of future observations. The analysis time of the first window starts at 2,400 s.

Figure 5 shows the analysis state RMSE curves of the different approaches. Let us examine first the RMSE evolution between the two configurations of Aug-EnVar and Aug-EnKF. Note that the assimilation window of Aug-EnVar is twice the length of Aug-EnKF. The errors of Aug-EnVar are smaller and grow slower than those of Aug-EnKF during the first half of the assimilation window of Aug-EnVar (which corresponds to the AugEnKF window) because the posterior state and parameter are not conditioned on future observations. During the second half of the Aug-EnVar assimilation window, Aug-EnVar yields greater errors compared to Aug-EnKF, but the slopes of the error curves remain comparatively the same. This indicates that the parameters are badly constrained due to a lack of smoothing effect. Again, as in Case I, this is due to an overfitting problem associated with the joint state/parameter estimation schemes.

In terms of the EnKF/EnRTS-EM method, the global RMSE trajectory recovered by the EM technique is clearly of better quality. The state errors at the observation time are slightly higher than the corresponding errors of Aug-EnVar/Aug-EnKF. Nevertheless, the evolution of state errors between two consecutive observations is characterized by a U-shaped curve, which suggests that the variance tensor is reasonably recovered by the EnKF/EnRTS-EM method. The overfitting phenomenon can thus be controlled or even avoided using this marginalized parameter estimation scheme. The quality of the variance tensor estimation is clearly improved with the EnKF/EnRTS-EM method.

The distinct RMSE evolution in terms of the different approaches can also be attributed to the estimated parameter profiles plotted in Figure 6. Note that the true parameter distribution is here unknown. We observe that the spatial distribution of the variance tensor for the Aug-EnKF method

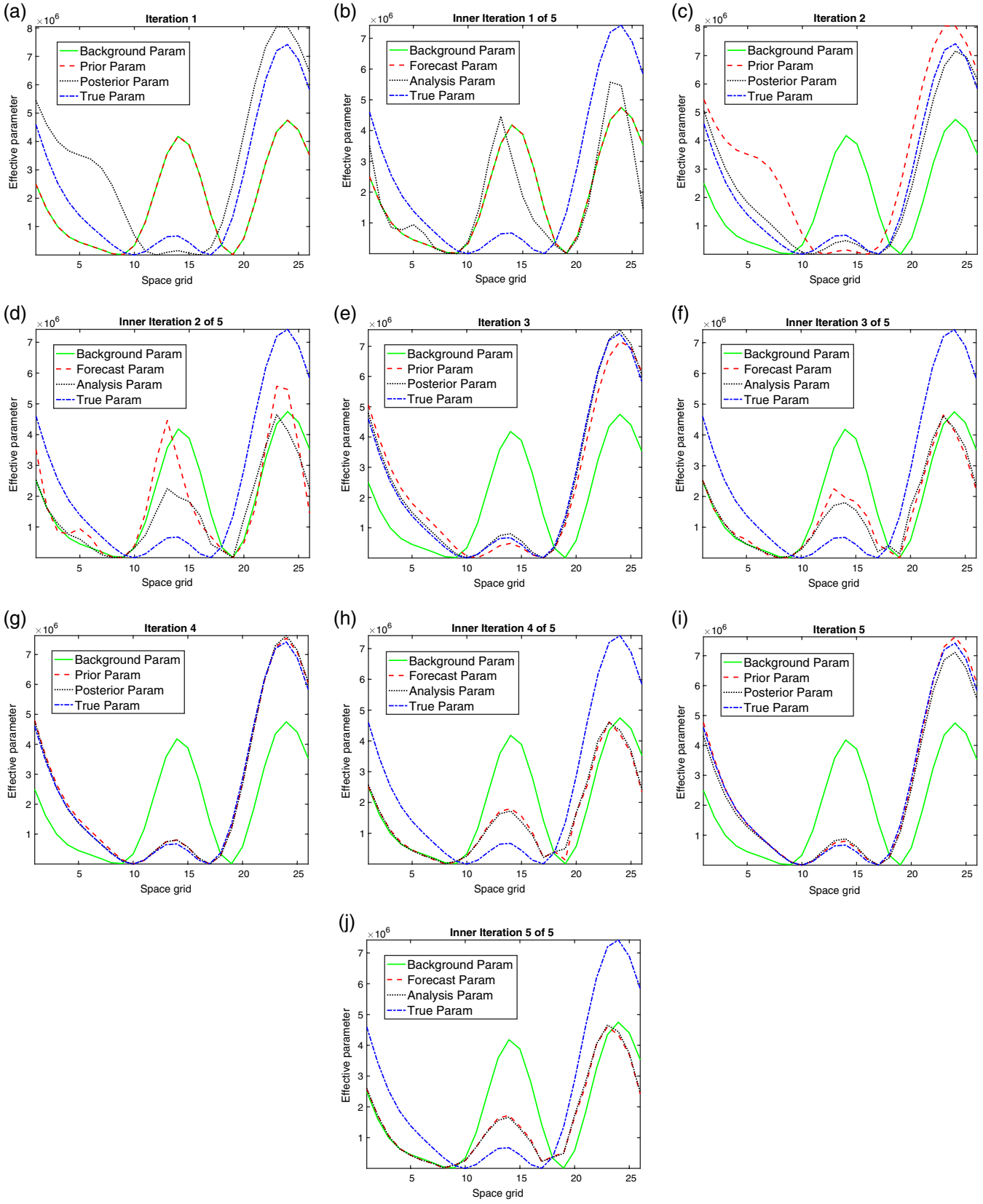

FIGURE 3 Case I: estimated parameter profile w.r.t. to iterations of EnKF/EnRTS-EM (left column, iterations 1 (a); 2 (c); 3 (e); 4 (g) and 5 (i)) compared to Aug-EnVar-EM (right column, iterations 1 (b); 2 (d); 3 (f); 4 (h) and 5 (j)) [Colour figure can be viewed at wileyonlinelibrary.com]

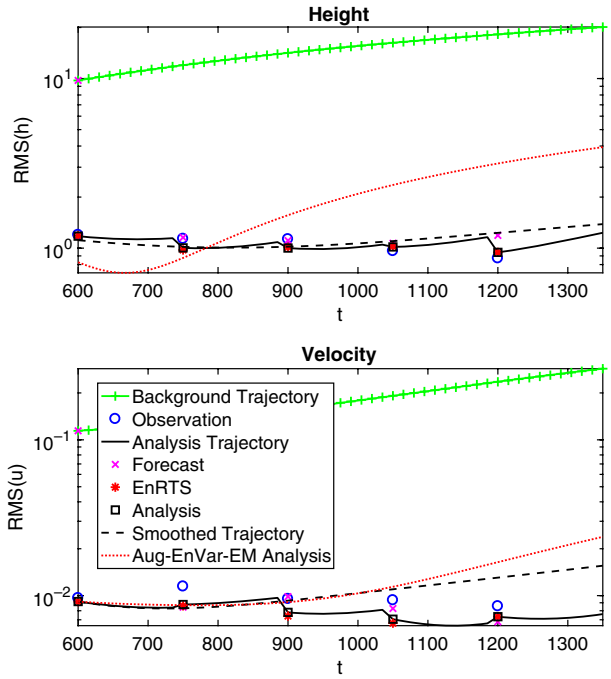

FIGURE 4 Case I: comparison of state RMSE evolution after the final EM iterations. Solid curve: the analysis trajectory yielded by EnKF within the E-step. Cross/Square: the forecast/analysis state yielded by EnKF in the E-step. Star: the smooth state yielded by the EnRTS smoother at the observation time. Dashed curve: the smooth trajectory yielded by integrating the initial smooth state using final estimated parameters. Dotted curve: the analysis trajectory yielded by Aug-EnVar-EM [Colour figure can be viewed at wileyonlinelibrary.com]

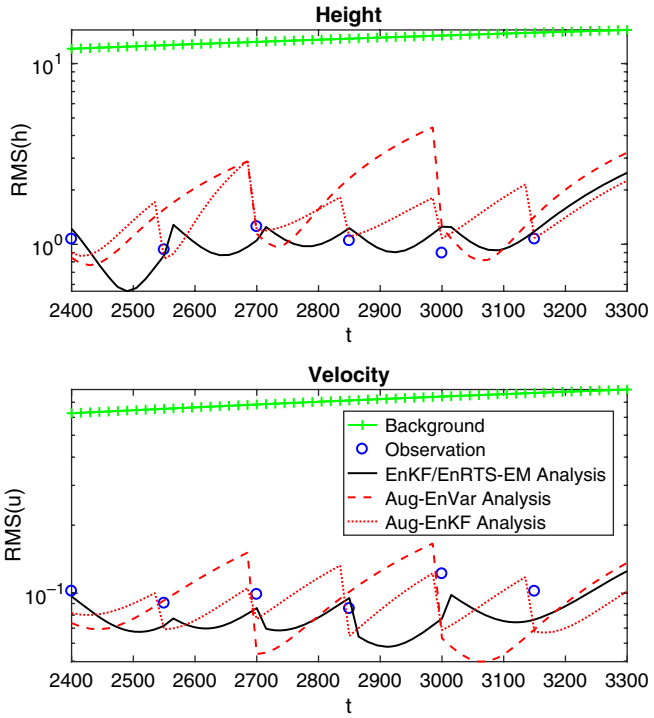

FIGURE 5 Case II: comparison of state RMSE evolution after the final EM iterations. Solid curve: the smooth trajectory yielded by integrating the initial smooth state after the final E-step using final estimated parameters after the final M-step. Dashed curve: the analysis trajectory yielded by Aug-EnVar-EM. Dotted curve: the analysis trajectory yielded by Aug-EnKF-EM [Colour figure can be viewed at wileyonlinelibrary.com]

is characterized by high-frequency fluctuations. This finding corresponds to our expectations, since the smoothing procedure in both Aug-EnVar and EnKF/EnRTS-EM tends to filter out those small-scale variations. The variance tensor obtained from Aug-EnVar exhibits higher values at the boundary. This helps to introduce extra forcing into the system and eventually reduces the state estimation error. The variance tensor resulting from EnKF/EnRTS-EM, on the other hand, shows a smaller magnitude and a longer correlation, both of which enable us to achieve flatter RMSE curves with slow-growing errors. This is likely due to the large magnitude of the variance tensor as well as of its gradient, which may trigger numerical instability associated with strong noise. However, the forecast quality starting at 3,150 s is not clearly improved by the EM approach. To improve the forecast, some sort of prediction of the parameter should probably be introduced. Learning procedures for the parameter's dynamics would be worth studying; however it is clearly a research topic in itself and we leave it for future exploration.

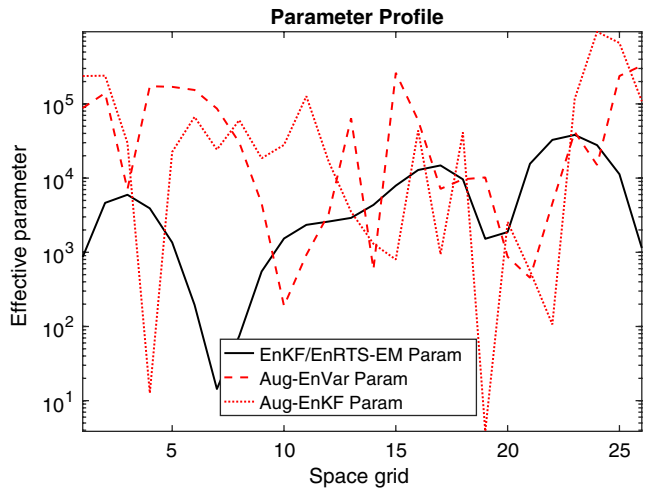

FIGURE 6 Case II: estimated parameter profile yielded from the window starting at 3,000 s [Colour figure can be viewed at wileyonlinelibrary.com]

9 | CONCLUSIONS

Recovering the exact parameters helps to compensate for errors due to approximations made in the analytical and/or numerical constitution steps of the geophysical dynamics models. To address this issue, a new parameter estimation scheme is proposed in this paper. This scheme is based on an ensemble formulation of both the E-step and the M-step of the EM algorithm.

The EM technique (McLachlan and Krishnan, 2007) offers an elegant and flexible solution for estimating the state and the model parameters separately. This method has been extensively used in many research domains, such as machine learning and system identification. Studies on integrating

the EM algorithm into a data assimilation framework have been considered only very recently. Dreano *et al.* (2017) and Pulido *et al.* (2018), among others, proposed applying the EM algorithm to the estimation of low-order model error covariance terms associated with a reduced-order noisy dynamics.

Unlike previous studies, our ensemble formulation of EM enables one to identify the *physical* subgrid parameter of a fluid dynamics model. This formulation extends the power of the EM algorithm to complex dynamical model identification problems that are quite common in geophysical dynamics modelling. Under these circumstances, we are more interested in finding the explicit parameter (with a possible spatial distribution) than a partially informative model error covariance that is not only cumbersome to compute but also far less representative of the real physics. Besides, direct parameter estimation obviates the auxiliary resampling procedure used to add random forcing during simulation. In the traditional setting, the EM algorithm is not really applicable to such problems, as closed-form expressions for the parameter update do not exist in general. Key to the proposed scheme is the use of an ensemble of ensembles in the maximization step to compute the sensitivity matrix of the error discrepancy with respect to the physical parameters. Boosted by this ensemble trick, the proposed scheme is able to tackle the estimation of high-dimensional parameters. Our ensemble-based EM algorithm can also be used to estimate the error covariance terms in a similar way to other EM algorithms but with an extended criterion. We have indeed shown that the ensemble-based covariance update scheme proposed in Dreano *et al.* (2017) corresponds to an approximation of our scheme.

In this paper, we focused on the identification from high-resolution observations of the model errors associated with unknown small-scale physical processes. The effect of these unresolved processes on the large-scale (resolved, coarse resolution) components must be properly parameterized through a subgrid-scale stress model. Within the stochastic flow dynamics framework proposed in Mémin (2014), such subgrid-scale stress models take the form of a diffusion term together with a corrective stochastic advection term. The subgrid model parameters are entirely controlled by the noise variance tensor, which is thus the quantity to be inferred from the data.

Our goal was therefore focused on evaluating the performance of the proposed EM algorithm to retrieve as accurately as possible such subgrid model parameters from high-resolution observations. This technique has been compared to an augmented state technique built from an EnVar method (Yang and Mémin, 2017). This latter technique supplied a sufficiently accurate reconstruction of the state, but provided a far less accurate parameter field, with the need for further retuning by an ad hoc inflation technique to avoid model blow-up and/or ensemble collapse.

The proposed EnKF/EnRTS-EM scheme has been shown to overcome the shortcomings associated with augmented-state-based techniques. The twin experiment designed here consists of two cases: the first case corresponds to a typical state and parameter estimation problem where the true stochastic parameter distribution is known, while the second case corresponds to the estimation of an optimum stochastic parameterization to represent the resolution-induced error associated with the scale discrepancy between the model and the data. For the first case, the proposed EnKF/EnRTS-EM scheme was able to retrieve the parameter profile with substantially higher accuracy than the augmented state techniques. For both cases, the proposed EnKF/EnRTS-EM scheme outperformed the augmented state techniques with regard to the forecast errors, and yielded better quality of both the estimated state and the parameters. Note that for the second case, the variance tensor was varying in time. To solve this problem, a quasi-online version of the EnKF/EnRTS-EM scheme has been implemented.

Although the proposed EnKF/EnRTS-EM scheme is very promising, concerns may be raised regarding the computational cost associated with the introduction of an ensemble of ensembles in the M-step. However, the introduction of certain mechanisms allowed us to compute an accurate ensemble-based evaluation of the cost function gradient with respect to the unknown parameter. Highly parallelized implementations as well as a more efficient optimization algorithm can be further explored to reduce the computational burden and keep the same accuracy in the model error characterization.

ACKNOWLEDGEMENTS

Yin Yang would like to thank Yu Zheng for drawing the attention to the EM algorithm. The authors thank the anonymous reviewers for their constructive comments.

ORCID

Yin Yang http://orcid.org/0000-0002-7492-8552

REFERENCES

Anderson, J.L. (2001) An ensemble adjustment Kalman filter for data assimilation. *Monthly Weather Review*, 129(12), 2884–2903.

Bishop, C.M. (2006) *Pattern Recognition and Machine Learning*. New York: Springer.

Chandramouli, P., Heitz, D., Laizet, S. and Mémin, E. (2018) Coarse large-eddy simulations in a transitional wake flow with flow models under location uncertainty. *Computers & Fluids*, 168, 170–189.

Chapron, B., Dérian, P., Mémin, E. and Resseguier, V. (2018) Large-scale flows under location uncertainty: a consistent stochastic framework. *Quarterly Journal of the Royal Meteorological Society*, 144(710), 251–260.

Cosme, E., Verron, J., Brasseur, P., Blum, J. and Auroux, D. (2012) Smoothing problems in a Bayesian framework and their linear Gaussian solutions. *Monthly Weather Review*, 140(2), 683–695.

Cotter, C., Gottwald, G. and Holm, D. (2017) Stochastic partial differential equations as a diffusive limit of deterministic Lagrangian multi-time dynamics. *Proceedings of the Royal Society A*, 473(2205), 20170388.

Delsole, T. and Yang, X. (2010) State and parameter estimation in stochastic dynamical models. *Physica D*, 239(18), 1781–1788.

Dreano, D., Tandeo, P., Pulido, M., Ait-El-Fquih, B., Chonavel, T. and Hoteit, I. (2017) Estimating model-error covariances in nonlinear state-space models using Kalman smoothing and the expectation–maximization algorithm. *Quarterly Journal of the Royal Meteorological Society*, 143(705), 1877–1885.

Evensen, G. (2003) The Ensemble Kalman Filter: theoretical formulation and practical implementation. *Ocean Dynamics*, 53(4), 343–367.

Gaspari, G. and Cohn, S.E. (1999) Construction of correlation functions in two and three dimensions. *Quarterly Journal of the Royal Meteorological Society*, 125(554), 723–757.

Haykin, S. (2004) *Kalman Filtering and Neural Networks*. New York: John Wiley & Sons.

Holm, D. (2015) Variational principles for stochastic fluid dynamics. *Proceedings of the Royal Society A*, 471(2716), 20140963.

Jordan, M.I. (2003) *An Introduction to Probabilistic Graphical Models*. unpublished, chapters available online. https://people.eecs.berkeley.edu/∼jordan/prelims/chapter11.pdf.

Kadri Harouna, S. and Mémin, E. (2017) Stochastic representation of the Reynolds transport theorem: revisiting large-scale modeling. *Computers & Fluids*, 156, 456–469.

Kraichnan, R. (1968) Small-scale structure of a scalar field convected by turbulence. *Physics of Fluids*, 11(5), 945–963.

Kraichnan, R. (1994) Anomalous scaling of a randomly advected passive scalar. *Physical Review Letters*, 72(7), 1016–1019.

Majda, A. and Kramer, P. (1999) Simplified models for turbulent diffusion: theory, numerical modelling, and physical phenomena. *Physics Reports*, 314(4–5), 237–574.

McLachlan, G. and Krishnan, T. (2007) *The EM Algorithm and Extensions*. *Wiley Series in Probability and Statistics*. Hoboken, NJ: John Wiley & Sons.

Mémin, E. (2014) Fluid flow dynamics under location uncertainty. *Geophysical and Astrophysical Fluid Dynamics*, 108(2), 119–146.

Navon, I. (1998) Practical and theoretical aspects of adjoint parameter estimation and identifiability in meteorology and oceanography. *Dynamics of Atmospheres and Oceans*, 27(1), 55–79.

Nelson, A.T. (2000) *Nonlinear estimation and modeling of noisy time-series by dual Kalman filtering methods*. PhD Thesis, Oregan Graduate Institute of Science and Technology..

Pulido, M., Tandeo, P., Bocquet, M., Carrassi, A. and Lucini, M. (2018) Stochastic parameterization identification using ensemble Kalman filtering combined with maximum likelihood methods. *Tellus A: Dynamic Meteorology and Oceanography*, 70(1), 1442099.

Raanes, P.N. (2016) On the ensemble Rauch–Tung–Striebel smoother and its equivalence to the ensemble Kalman smoother. *Quarterly Journal of the Royal Meteorological Society*, 142(696), 1259–1264.

Resseguier, V., Mémin, E. and Chapron, B. (2017a) Geophysical flows under location uncertainty, Part I: random transport and general models. *Geophysical & Astrophysical Fluid Dynamics*, 111(3), 149–176.

Resseguier, V., Mémin, E. and Chapron, B. (2017b) Geophysical flows under location uncertainty, Part II: quasi-geostrophy and efficient ensemble spreading. *Geophysical & Astrophysical Fluid Dynamics*, 111(3), 177–208.

Resseguier, V., Mémin, E. and Chapron, B. (2017c) Geophysical flows under location uncertainty, Part III: SQG and frontal dynamics under strong turbulence conditions. *Geophysical & Astrophysical Fluid Dynamics*, 111(3), 209–227.

Resseguier, V., Mémin, E., Heitz, D. and Chapron, B. (2017d) Stochastic modelling and diffusion modes for proper orthogonal decomposition models and small-scale flow analysis. *Journal of Fluid Mechanics*, 826, 888–917.

Sondergaard, T. and Lermusiaux, P.F.J. (2013) Data assimilation with Gaussian mixture models using the dynamically orthogonal field equations. Part I: theory and scheme. *Monthly Weather Review*, 141(6), 1737–1760.

Sura, P., Newman, M., Penland, C. and Sardeshmukh, P. (2005) Multiplicative noise and non-Gaussianity: a paradigm for atmospheric regimes? *Journal of the Atmospheric Sciences*, 62(5), 1391–1409.

Ueno, G. and Nakamura, N. (2014) Iterative algorithm for maximum-likelihood estimation of the observation-error covariance matrix for ensemble-based filters. *Quarterly Journal of the Royal Meteorological Society*, 140(678), 295–315.

Ueno, G. and Nakamura, N. (2016) Bayesian estimation of the observation-error covariance matrix in ensemble-based filters. *Quarterly Journal of the Royal Meteorological Society*, 142(698), 2055–2080.

Yang, Y. and Mémin, E. (2017) High-resolution data assimilation through stochastic subgrid tensor and parameter estimation from 4DEnVar. *Tellus A: Dynamic Meteorology and Oceanography*, 69(1), 1308772.

Yang, Y., Robinson C, Heitz, D. and Mémin, E. (2015) Enhanced ensemble-based 4DVar scheme for data assimilation. *Computers & Fluids*, 115, 201–210.

How to cite this article: Yang Y, Mémin E. Estimation of physical parameters under location uncertainty using an ensemble^2–expectation–maximization algorithm. *Q J R Meteorol Soc.* 2019;145:418–433. https://doi.org/10.1002/qj.3438